第 49 卷 第 10 期/2022 年 5 月/中国激光 特邀综述

中国激光

超短脉冲激光加工在微电/光互连领域的应用研究进展

孙小燕[1,2]，梁昶[1,2]，张伟[1,2]，孔德键[1,2]，冯玉婷[1,2]，胡友旺[1,2*]，段吉安[1,2]

[1]中南大学机电工程学院，湖南 长沙 410083；

[2]高性能复杂制造国家重点实验室，湖南 长沙 410083

摘要 超短脉冲激光凭借其脉宽窄、峰值功率高的特点，可以实现高精度材料生长、改性和去除等形式的加工，具有良好的材料适应性和工艺兼容性，在微电/光互连领域取得了开拓性应用进展，已成为近年来先进制造的新兴关键技术。本文简要介绍超短脉冲激光实现微光电子器件制造的基本机制，包括多光子还原、表面等离子体共振和双光子聚合等，重点阐述超短脉冲激光加工在微光/电互连领域的应用研究进展，并对超短脉冲激光加工在该领域的发展方向进行总结和展望。

关键词 激光技术；超短脉冲激光；多光子还原；表面等离子体共振；双光子聚合；光波导

中图分类号 TN249 **文献标志码** A **DOI**：10.3788/CJL202249.1002502

1 引 言

随着科技的进步，电子和信息器件不断向便携化、微型化和智能化方向发展，器件功能单元高密度分布，这对功能单元间的电互连[1-2]和光互连[3]技术提出了新需求，甚至是严峻挑战。金属纳米线，如银、金和铜纳米线，因结构尺寸小，在微电互连应用方面具有独特优势，但其高性能制备工艺尚不成熟，且由于纳米线之间的接触电阻较大，未经过焊接处理的金属纳米线网格通常表现出较差和不均匀的导电性[4-7]。此外，随着光芯片的发展，光芯片间的耦合、传输需求也刺激着光互连技术的发展。光互连根据其传输信道不同，可分为光纤互连、波导互连和自由空间光互连。由于芯片间或者芯片内的光互连尺寸相对较小，因此波导互连的应用最为广泛[8]。虽然电互连与光互连可以分别实现不同的功能，但随着器件集成度的提高，光/电和电/光转换模块已广泛使用，从而必将促进光/电互连技术的发展。目前，连接已由宏观尺度发展到微纳空间尺度，如何实现高质量、低损伤和高可靠性的电/光互连已成为研究热点之一。

以亚微米量级电/光互连为例，为避免对周围材料的影响，加工能量需要精确聚集。高能束因其能量可被精确控制而最早被用于波导[9]与碳纳米管[10]的互连。飞秒激光加工由于具有无需真空环境、非接触、加工灵活、加工材料类型广及冷加工等优点，近年来在超精密加工领域得到了广泛应用，尤其是在电/光互连领域，它可以实现金属、透明介质等材料在零维到三维的加工，涉及的加工机制包括光还原[11]、等离子体共振[12-13]和双光子聚合[14]等。本文将从超短脉冲激光与物质相互作用机制出发，综述其在微光/电互连领域的应用研究进展，并对超短脉冲激光加工在该领域的发展方向进行总结和展望。

2 超短脉冲激光互连加工机制

2.1 光化学还原

光化学还原法是利用材料与飞秒激光相互作用过程中的多光子吸收效应还原前驱体溶液，实现零维材料的制备和电连接。以金前驱体为例，其多光

收稿日期：2021-12-01；**修回日期**：2022-01-11；**录用日期**：2022-01-19

基金项目：国家自然科学基金(51875584，51875585)、电子元器件可靠性物理及其应用技术重点实验室开放基金(20D10)、湖南省自然科学基金(2020JJ4247)

通信作者：*huyw@csu.edu.cn

子还原主要有三个过程[11,15-17]：(Ⅰ)水通过多光子吸收产生自由电子和自由基，如式(1)～(3)所示；(Ⅱ)金离子通过电子和自由基还原为金原子，如式(4)～(7)所示；(Ⅲ)金原子团聚形成金纳米颗粒，如式(8)所示。

水对飞秒激光的多光子吸收(Ⅰ)：

$$H_2O \xrightarrow{nh\nu} H_2O^+ + e^-(n \geqslant 2), \tag{1}$$

$$H_2O^+ + H_2O \rightarrow H_3O^+ + OH\cdot, \tag{2}$$

$$H_3O^+ + e^- \rightarrow H_2O + H\cdot。 \tag{3}$$

金原子的还原(Ⅱ)：

$$Au^{3+} + H\cdot \rightarrow Au^{2+} + H^+, \tag{4}$$

$$Au^{3+} + e^- \rightarrow Au^{2+}, \tag{5}$$

$$Au^{2+} + Au^{2+} \rightarrow Au^{3+} + Au^+, \tag{6}$$

$$Au^+ + e^- \rightarrow Au^0。 \tag{7}$$

金原子的团聚(Ⅲ)：

$$mAu^0 \rightarrow (Au^0)_m。 \tag{8}$$

2.2 激光诱导表面等离子体共振效应

当超快激光辐照在纳米颗粒或纳米线上时，会产生表面等离子体共振，光场分布局域增强。同时，局部等离子体共振会产生天线效应，使更大区域的光会聚到增强区域，在等离子体共振处产生热点。这种效应使得两个或多个纳米结构界面附近会选择性地产生局部软化或熔化而形成连接，且对周围结构无附带热损伤，当连接完成后局域增强场就会减弱。通过飞秒激光诱导表面等离子体共振可以实现零维纳米颗粒、一维纳米线和纳米管、二维石墨烯等材料的电互连。

2.3 超快激光诱导折射率变化

透明介质对聚焦飞秒激光的能量吸收、电离过程是一个非线性过程，通过多光子电离、隧穿效应和雪崩电离等机制产生载流子激发，当载流子浓度达到临界值时，等离子体频率达到激光频率形成共振。此后，材料对激光的吸收能力急剧增强，易使材料形成光损伤，导致其性质(如折射率)发生改变。折射率的变化机制与加工材料、工艺参数有关，目前的机制主要包括：1)材料致密化导致折射率增大；2)材料黏流化温度变化导致折射率增大(反常黏流化温度行为)或减小(正常黏流化温度行为)；3)色心缺陷；4)光折变和离子重分布使折射率增大或减小。通过飞秒激光诱导折射率变化，可以实现光波导的加工。

2.4 双光子聚合

双光子聚合是指在激光辐照下，液态单体材料中的价带电子同时吸收两个光子发生能级跃迁，液态单体材料经过聚合和交联反应形成固态产物的过程。双光子吸收是一种典型的三阶非线性光学效应，仅在光强足够大的情况下发生。飞秒激光聚焦后的高能量密度可以实现双光子聚合，可应用于光互连。

3 超短脉冲激光加工在微电互连领域的应用

3.1 零维导电材料的制备与互连

导电材料根据其结构可分为零维、一维和二维材料。常用的零维材料有纳米颗粒，一维材料有纳米棒和纳米线，二维材料主要有石墨烯等。目前，飞秒激光制备零维导电材料和实现材料互连的方法有多种，如多光子还原法、光动力组装法和烧结法。

3.1.1 多光子还原法制备导电材料

飞秒激光多光子还原法主要是利用超短脉冲宽度和高峰值功率的飞秒激光与前驱体溶液发生非线性作用，将金属离子还原成金属原子，原子团聚形成纳米颗粒。由于多光子吸收的空间范围与多光子吸收个数的平方根呈反比，因此，这种加工方法可以突破光学衍射极限，加工分辨率可达亚微米量级。此外，飞秒激光诱导多光子还原法针对的是金属前驱体溶液，因此具有较高的加工灵活性，可以实现二维和三维导电结构的加工。

如图 1 所示，研究人员采用双光子还原法在硝酸银溶液中制备了银纳米颗粒，加工分辨率可达 1.02 μm，颗粒堆积组成纳米线，实现了电极间的互连。实测银导线的电阻率为 5.30×10^{-8} Ω·m，仅为银的 3.3 倍[18]。然而，由于加工过程中存在热效应，易发生氧化反应和产生气泡，因此难以达到亚微米级加工。为降低热效应，在反应溶液中添加适量的光敏染色剂香豆素 400 辅助多光子还原，可使银纳米颗粒的加工分辨率提高到 400 nm，并实现 120 μm×120 μm 银线网格的高效加工，对亚微米级电互连具有重要意义。在还原金的过程中以 ruthenium(II) tris(bipyridine)作为光引发剂，可将金纳米颗粒尺寸控制在 50～200 nm 量级，其导线的电阻率约为 2×10^{-7} Ω·m[19]。

在前驱体溶液中添加表面活性剂可以提高多光子还原法的加工分辨率。例如，通过控制表面活性剂的浓度、分子结构等参数，可以抑制纳米颗粒的团聚，从而提高加工分辨率。Cao 等[20]利用癸酰基肌氨酸钠(NDSS)作为银离子生长的抑制剂，降低了

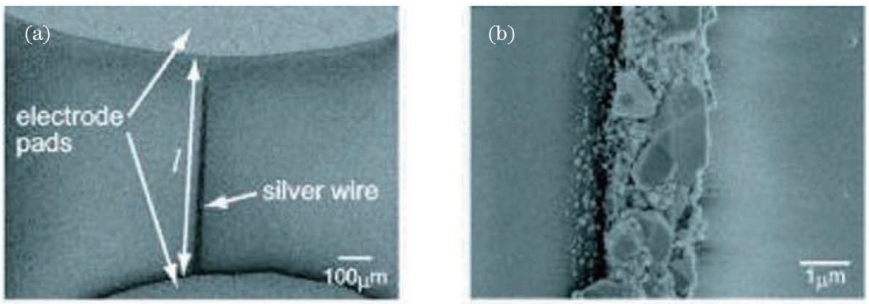

图 1 多光子还原实现电连接[18]。(a)银纳米导线与电极的电镜图;(b)银纳米导线的高倍电镜图

Fig. 1 Multiphoton reduction to achieve electrical connection. (a) Electron microscopy of silver nanowires and electrodes; (b) high magnification electron microscopy of silver nanowires

银纳米颗粒的聚集效应;同时他们发现,当 NDSS 的浓度大于临界值时,可以获得更高的加工分辨率和更好的加工连续性。Cao 等[21]利用脂肪酸盐辅助成功还原了金属纳米颗粒,他们通过增加脂肪酸盐中的碳链长度,减小了银纳米颗粒的特征尺寸,提高了加工精度。Lu 等[22]采用末端氨基离子液辅助多光子还原实现了金的亚波长分辨率加工,最小加工尺度为 228 nm,长度为 75 μm,电阻率约为 1.65×10^{-7} Ω·m;此外,他们利用该技术实现了多电极直写加工,如图 2 所示。Ren 等[23]研究了甘氨酸和亮氨酸等在多光子还原纳米银颗粒过程中的作用,结果发现,还原的银纳米线的最小直径为 186 nm,最小电阻率为 4.1×10^{-7} Ω·m(为银块体的 25 倍)。

虽然利用表面活性剂可以降低光还原金属颗粒的尺寸,但残留的活性剂会降低结构的导电性能。柠檬酸钠在水溶液中具有较大的溶解度,在完成光还原后,柠檬酸钠可以被去除。Xu 等[24]在柠檬酸

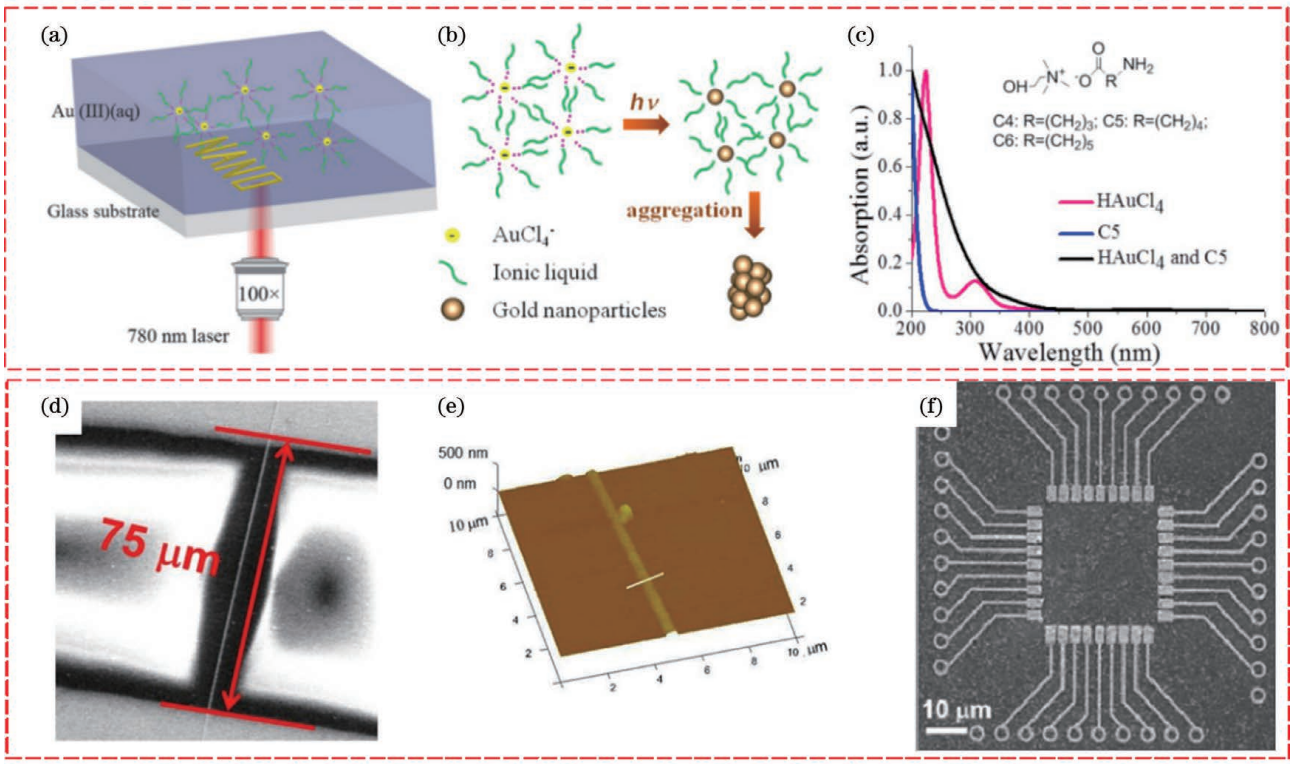

图 2 表面活性剂辅助飞秒激光实现电连接[22]。(a)金纳米线还原示意图;(b)多光子还原金纳米颗粒的机制;(c)$HAuCl_4$、C5 及其混合液的吸收光谱;(d)金纳米线的 SEM 图;(e)金纳米线的 AFM 图;(f)微电路

Fig. 2 Electrical connection by femtosecond laser with assistant of surfactant[22]. (a) Schematic of gold nanowire reduction; (b) mechanism of multiphoton reduction of gold nanoparticles; (c) absorption spectra of $HAuCl_4$, C5, and their mixture; (d) SEM image of gold nanowires; (e) AFM diagram of gold nanowires; (f) image of microcircuits

钠和硝酸银混合溶液中直写了宽为 80 nm 的银纳米线，实现了 Au-Ge-Ni 电极的互连，该导线的电阻率约为 1.7×10^{-7} Ω·m。但这种加工方法仍存在离子扩散的问题，降低了加工质量。为了解决金属离子在焦点处局部损耗的问题，Xu 等[24]提出了在银前驱体中掺杂平均直径为 10 nm 银颗粒的方法。与纯银前驱体相比，这种方法仅需原 1/10 的激光功率即可实现连续图案的加工，所加工结构的表面粗糙度为 6 nm。Xu 等利用这种方法加工出了双 T 形电极，电极的宽度为 100 μm，电阻率为 2.31×10^{-7} Ω·m[1]。

在飞秒激光直写过程中，前驱体溶液中的金属离子易扩散，从而导致加工不均匀。为了解决这一问题，研究人员尝试在聚合物基质内进行了电连接，这种方法可以防止金属离子扩散[25]。Baldacchini 等[26]提出了在聚乙烯吡咯烷酮(PVP)内部还原银纳米线的方法，但该方法还原出的纳米线不连续，导致电阻率增大。Maruo 等[27]通过提高激光能量和银离子浓度，在玻璃基底上实现了连续银纳米导线的制备，其最小直径约为 1.7 μm，如图 3(a)所示，电阻率可降低至 3.48×10^{-7} Ω·m。

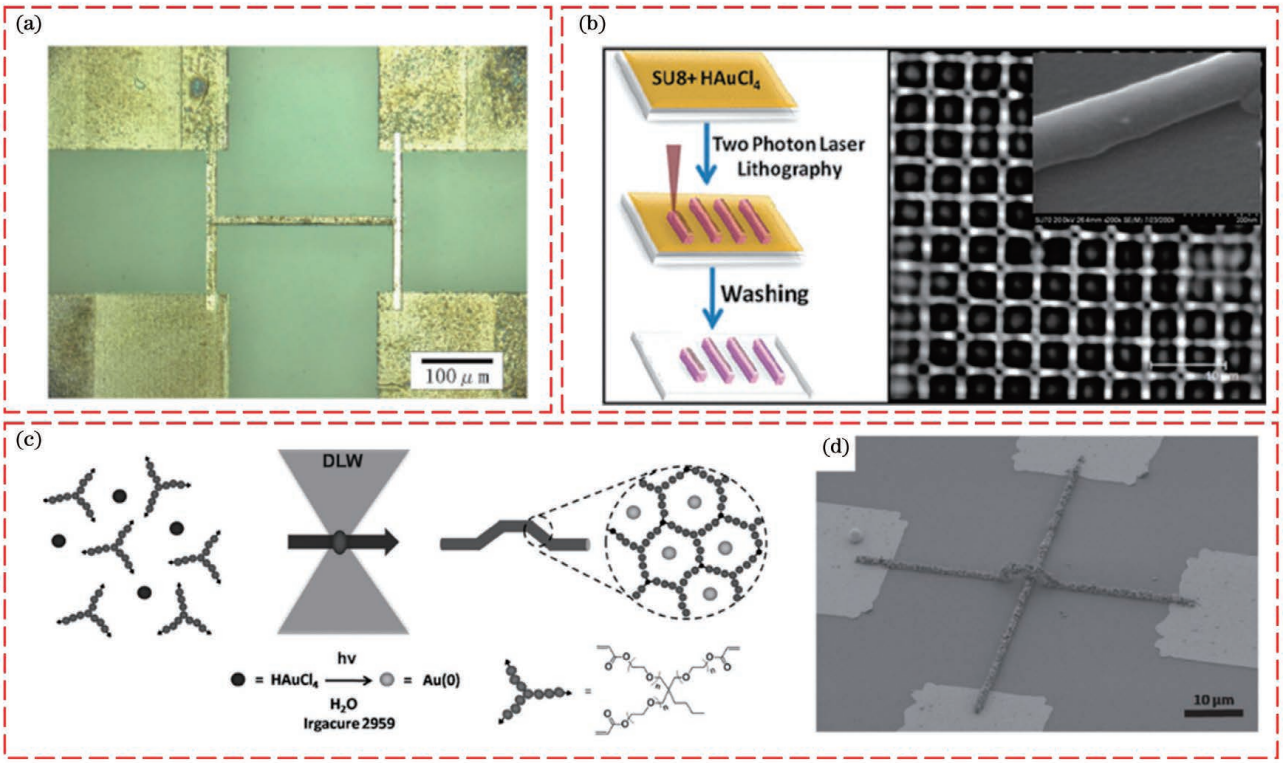

图 3 在聚合物内实现电连接。(a)在 PVP 内部实现金电极互连[27]；(b)在掺杂 Au^{3+} 的 SU8 中还原金纳米导线[28]；(c)在复合光刻胶中还原金纳米颗粒[29]；(d)在复合光刻胶中实现 3D 电连接[29]

Fig. 3 Electrical connection is achieved within polymer matrix. (a) Gold electrode interconnection within PVP[27]; (b) reduction of gold nanowires in SU8 doped with Au^{3+} [28]; (c) reduction of gold nanoparticles in composite photoresist[29]; (d) 3D electrical connection in composite photoresist[29]

Shukla 等[28]在亚波长分辨率聚合物基体中制备了高导电金纳米导线，如图 3(b)所示；他们利用飞秒脉冲激光将纳米结构直接写入掺杂金前驱体的光刻胶 SU8 中，同时利用飞秒激光诱导多光子还原和双光子聚合效应，制备了宽度为 800 nm 的金导线，其最大电阻率仅为金的 4 倍。Blasco 等[29]开发了一种掺杂光引发剂 2959 的复合光刻胶，同时结合退火工艺，制备了连续性较好的纳米导线，其电阻率为 4.5×10^{-7} Ω·m，约为金的 20 倍。除此之外，Blasco 等[29]还利用这种方法实现了电极的三维互连，如图 3(c)、(d)所示。Hu 等[30]将季戊四醇三丙烯酸酯(PETA)与金前驱体混合，利用双光子聚合和多光子光还原法制备了复杂的三维金纳米复合结构(纳米线的最小宽度为 78 nm)，该技术在飞秒激光三维电互连领域具有广阔的应用前景。

3.1.2 光动力法组装电极

尽管多光子还原法具有较高的加工精度和灵活性，但其存在焦点处金属离子迁移速度低的问题。当焦点处的金属离子耗尽时，焦点处的金属离子便难以得到补充，从而影响了加工质量。为了解决这

一问题，研究人员提出了光动力组装法，即：在高浓度的金属胶体中，利用光驱动力对金属种子进行捕获，实现纳米结构的加工。与多光子还原法相比，该方法的优势是利用高浓度金属胶体可以实现损耗的快速补充，并且，该方法无需表面活性剂即可实现高精度和高导电结构的加工。但是，目前飞秒激光动力组装法多局限于加工二维纳米导线。

Wang 等[31]通过紧聚焦飞秒激光实现了银纳米颗粒的自组装。在飞秒激光作用下，平均直径约为 2.5 nm 的银颗粒被聚集在光斑中心，并被激光烧结至基底上。该方法的加工分辨率可突破光学衍射极限，达到 190 nm。通过改变飞秒激光直写的路径，可以在基底上实现叉指电极、双电极和电极阵列的图案化加工，如图 4 所示。该方法加工的电极尺度达到了细胞级别，可用于细胞探测分析。陈忠赟等[32]利用相同的方法直写了银纳米线，其电阻率为 3.28×10^{-7} Ω·m，为银的 19.88 倍。与银电极相比，金电极更为稳定。Urban 等[33]利用 532 nm 飞秒激光的光驱动力实现了金纳米颗粒在胶体中的捕获，并驱动其至光斑中心位置，然后利用范德瓦耳斯力克服静电排斥力，实现了纳米颗粒的固定。Bahns 等[34]利用 488 nm 飞秒激光对直径为 50 nm 的金颗粒和碳颗粒进行组装，实现了 Au-C-Au 纤维的有机-无机多级纳米颗粒的组装，其电阻率为 2.33×10^{-6} Ω·m。Xu 等[2]利用光梯度力驱动金纳米颗粒聚集到光斑中心，实现了宽度为 560 nm 的金纳米线的加工，并将其应用于 Au-Ge-Ni 电极的互连；该金纳米线的电阻率为 5.5×10^{-8} Ω·m，仅为金的 2 倍。

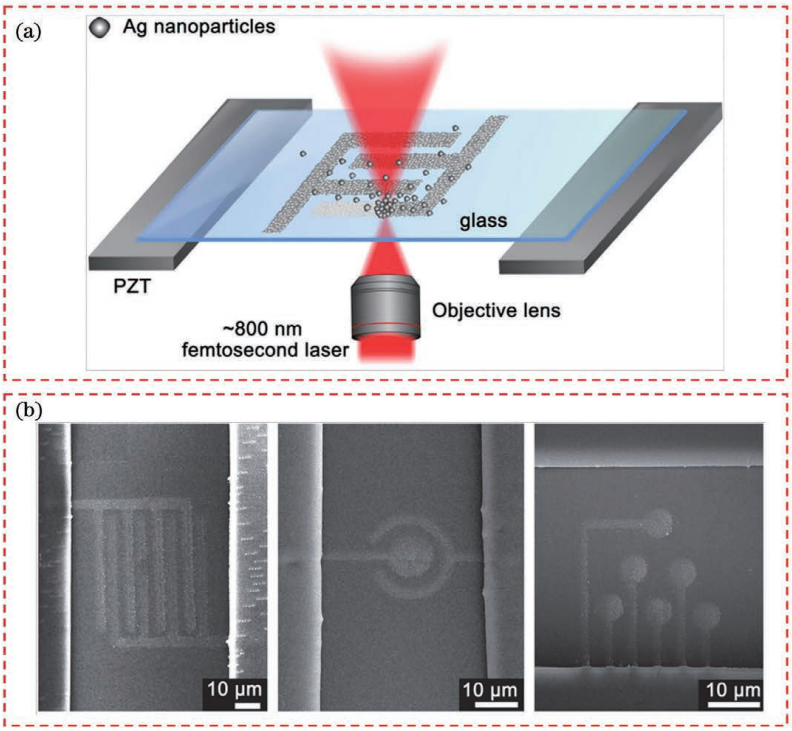

图 4 光动力组装法实现电连接[31]。(a)光动力组装法示意图；(b)光动力组装法实现叉指电极、双电极和多电极的加工

Fig. 4 Electrical connection is realized by photodynamic assembly method[31]. (a) Schematic of photodynamic assembly method; (b) fabrication of cross-finger electrodes, double electrodes, and multiple electrodes by photodynamic assembly method

3.1.3 烧结法加工电极

飞秒激光烧结主要是通过强激光激发金属纳米颗粒的等离子体共振效应来实现金属纳米颗粒的烧结。与多光子还原法和光动力组装法相比，飞秒激光烧结法不需要在液相环境下进行，有利于避免金属离子在组装过程中的扩散现象。由于尺度效应，金属纳米颗粒的熔点通常比其块体材料要低。通过控制飞秒激光的工艺参数，可对纳米颗粒的热场进行控制，实现纳米颗粒的精准烧结[35]。

银具有良好导电性和化学稳定性，是超短脉冲烧结法常选用的材料之一。Huang 等[36]采用低光通量(900 μJ/cm²)飞秒激光在硅片上实现了银纳米颗粒的无损烧结。但是，当光通量过大时，银纳米颗粒受飞秒激光辐照熔化后就会合并为大颗粒[37]。Son 等[38]提出了利用飞秒激光烧结纳米电极的方法，并用该方法实现了对银纳米颗粒熔化的选择性

控制，最小加工精度可突破衍射极限，达到 100 nm，所制备银导线的电阻率为 1.8×10^{-7} Ω·cm；此外，他们利用该方法加工了 p 型增强模型有机场效应管，实现了电路的开/关控制。然而，飞秒激光烧结的电极机械强度和导电性不足，需要对光通量进行优化。Noh 等[39]研究了光通量对银纳米颗粒烧结的影响，加工系统如图 5(a)所示。该研究者指出，低光通量有利于相邻银纳米颗粒的互连，随着光通量增加，纳米颗粒会发生熔化甚至球化，从而急剧降低了电极的机械强度。

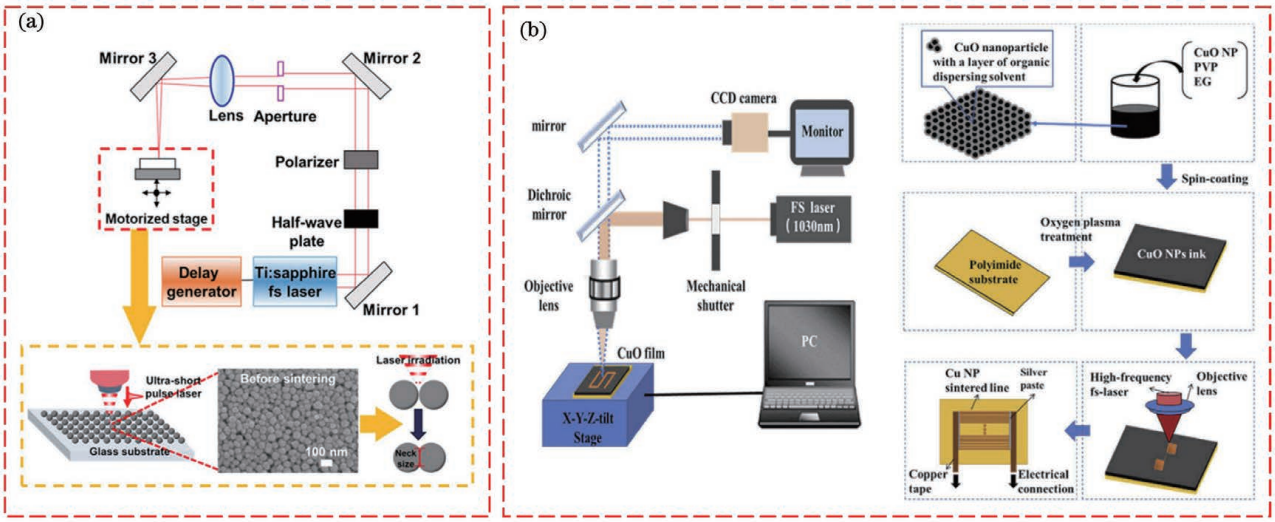

图 5 飞秒激光烧结纳米颗粒实现电连接。(a)飞秒激光烧结银纳米颗粒[39]；(b)飞秒激光烧结铜纳米颗粒[43]

Fig. 5 Electrical connection is realized by femtosecond laser sintering of nanoparticles. (a) Femtosecond laser sintering of silver nanoparticles[39]; (b) femtosecond laser sintering of copper nanoparticles[43]

铜是一种导电性好且价格较低的常用导电材料。Mizoshiri 等[40-41]利用飞秒激光还原性烧结 CuO 纳米颗粒，制备了铜基微温度探测器；随后，他们将 CuO/NiO 纳米颗粒烧结还原为 Cu/Ni 纳米颗粒，然后进行二次氧化烧结，得到了 Cu_2O/NiO 纳米颗粒。通过这种还原烧结方法，他们得到了 N 型和 P 型热电耦合器单元，器件的开路电压为 0.25 mV/K。廖嘉宁等[42]采用 800 nm 飞秒激光对铜纳米颗粒进行烧结，制备的铜电极的最小方块电阻为 11.2 $\Omega\cdot sq^{-1}$。Huang 等[43]利用频率为 76 MHz 的飞秒激光在聚酰亚胺(PI)薄膜上还原性烧结铜电极，如图 5(b)所示，他们通过优化扫描速度，得到了宽度为 5.5 μm、孔隙率为 9.89%的铜线，铜线的纯度达到了 91.42%，电阻率约为 1.3×10^{-7} Ω·m。铜易在空气中氧化，若在烧结过程中采用氮气或氩气保护，可防止铜的氧化[44]。

综上所述，飞秒激光实现零维材料的制备与电互连的方法主要有多光子还原法、光动力组装法和烧结法，这三种方法各有优势。多光子还原法的最大优势是可以实现三维导电结构的高精度加工，但目前制备的导电材料主要是贵金属。光动力组装法主要解决了金属离子的迁移问题，利用金属纳米胶体实现二维导电结构的加工。烧结法主要是在二维平面上实现电连接，可对铜和镍等金属进行加工，而不仅仅局限于贵金属加工。但烧结法目前需要解决的问题是加工过程中导电结构的氧化问题。需要指出的是，以上加工方法均存在加工效率低的问题，可采用光束整形的方法实现高效并行加工[45-46]。

3.2 导电材料的焊接

提高一维纳米导电材料之间导电性的连接技术包括机械应力法、焦耳热法、卤化物焊接法和光/激光辐照法等[4-5,47-49]。针对金属纳米线的连接，机械应力法较为复杂，并且因为压力不均容易破坏金属纳米线的强度；热处理法易损坏不耐高温的柔性衬底或银纳米线晶体结构；卤化物焊接法在提高薄膜导电性的同时会降低薄膜的光透过率；光辐照法工艺简单，焊接效率高，在特定工艺参数下可在热敏衬底上实现金属纳米线间的焊接。激光辐照焊接金属纳米线网络就是利用纳米材料与光波的相互作用来实现纳米材料之间的快速自限焊接。相比连续激光和纳秒脉冲激光，飞秒激光焊接的热效应小，焊接过程不会将纳米线和衬底材料整体加热，只是在银纳米线节点处产生局部场增强效应，软化节点处纳米线表面的晶格，实现纳米线的焊接[50-52]。

3.2.1 纳米线焊接的局域场增强机制

研究人员通过分析双光子诱导发光微光谱分布随飞秒激光波长的演变规律发现，在一维金纳米线末端和耦合的带隙区域，局域场强度在共振时比非共振时至少高一个数量级（图 6），证明了飞秒激光辐照会诱导金纳米线出现局部场增强[53]。飞秒激光辐照银纳米线同样也可以诱导局部等离子体共振，局部等离子体共振产生的局域高温可用于纳米线连接、切割和重塑。此外，由于热扩散使整体温度在 10^{-12} s 内达到平衡，因此局部等离子体共振之外的纳米线结构不会受高温影响而破坏。相关研究表明，当纳米线的共振波长与入射激光波长相匹配时，纳米线在电场增强区域开始熔化，对于单根银纳米线来说，这种增强和熔化首先发生在线的两端。研究人员利用时域有限差分法（FDTD）模拟了等离子体的电场分布，结果表明，激光偏振方向对等离子体能量分布和熔化过程有显著影响。当偏振垂直于纳米线长轴方向时，纳米线末端的局域电场增强明显，因而会首先熔化（图 7）[54]。

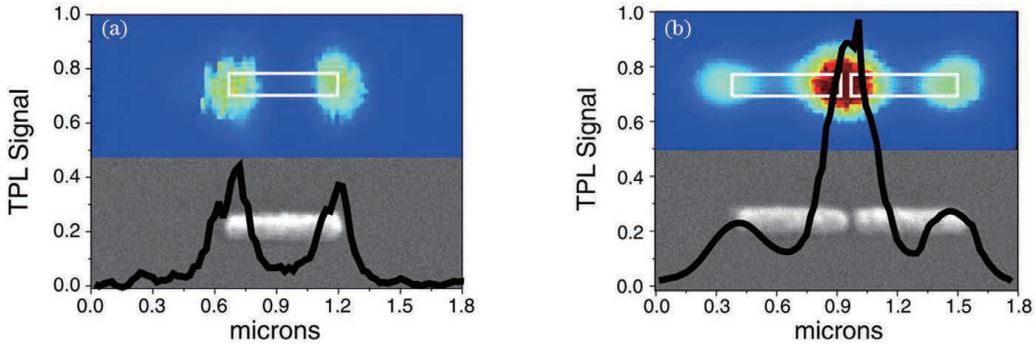

图 6 金纳米线的双光子诱导发光光谱及其对应的扫描电镜图[53]。(a)单根金纳米线；(b)耦合的金纳米线

Fig. 6 Two-photon induced luminescence spectra of gold nanowire and its corresponding SEM images[53]. (a) Single gold nanowire; (b) coupled gold nanowire

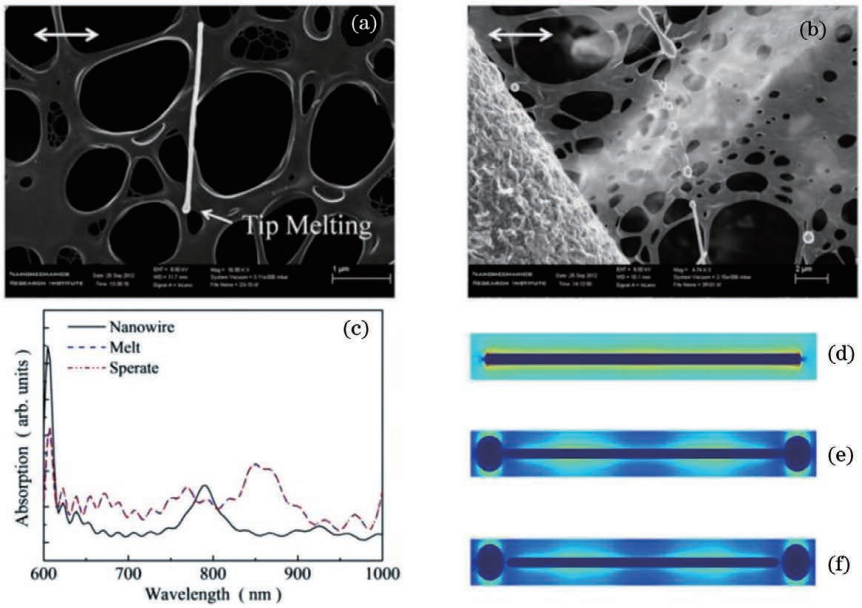

图 7 激光偏振垂直于银纳米线长轴时的纳米线熔化情况及电场强度分布[54]。(a)纳米线末端熔化，其中双向箭头表示激光偏振方向；(b)纳米线分散熔化，纳米线被分离成纳米粒子；(c)FDTD 模拟计算的吸收光谱；(d)FDTD 计算的电场强度分布；(e)银纳米线两端熔化后的电场强度分布；(f)纳米粒子从纳米线末端分离时的电场强度分布

Fig. 7 Melted nanowire and electric field intensity distributions when laser polarization is perpendicular to the long axis of silver nanowire[54]. (a) Melting of nanowire ends, where the double sides arrow indicates the laser polarization direction; (b) the nanowire is dispersed and melted, and the nanowire is separated into nanoparticles; (c) absorption spectrum calculated by FDTD simulation; (d) electric field distribution calculated by FDTD; (e) electric field intensity distribution after silver nanowire melting on both ends; (f) electric field intensity distribution after nanoparticles separate from the ends of the nanowire

3.2.2 同质纳米线互连

如图 8(a)、(b)所示，利用飞秒激光辐照诱导银纳米线局部等离子体共振效应，通过调控飞秒激光脉冲的辐照能量，在不添加填充材料的情况下可以将空间分离的银纳米线成功连接起来，形成 Y 形和 T 形纳米线结构。纳米连接就是相邻纳米线间隙附近产生了高度局部化的热量，两根纳米线端部均发生熔化而流入间隙形成连接。研究人员发现，焊接接头的形成与纳米线长轴之间的夹角、距离有关，通过调节入射激光的偏振方向和优化激光能量，可以控制近间隙区纳米金属的熔化[12,55]。同样，飞秒激光也可以诱导银纳米粒子在银纳米线上组装形成周期性阵列。银纳米线与硅衬底接触后，纳米线-硅界面电场的增强对附近银纳米粒子有显著的吸引作用，因此，纳米线表面以及纳米线-硅界面处的电场分布高度依赖于激光偏振。当偏振方向与纳米线的长轴平行时，有利于纳米粒子的有序排列；当银纳米线的长度超过激光波长的两倍时，纳米线的排列有序性变差，然而，银纳米颗粒在长纳米线上仍然存在自组装现象。研究表明，纳米线与硅衬底之间也会产生局部场增强[56]。

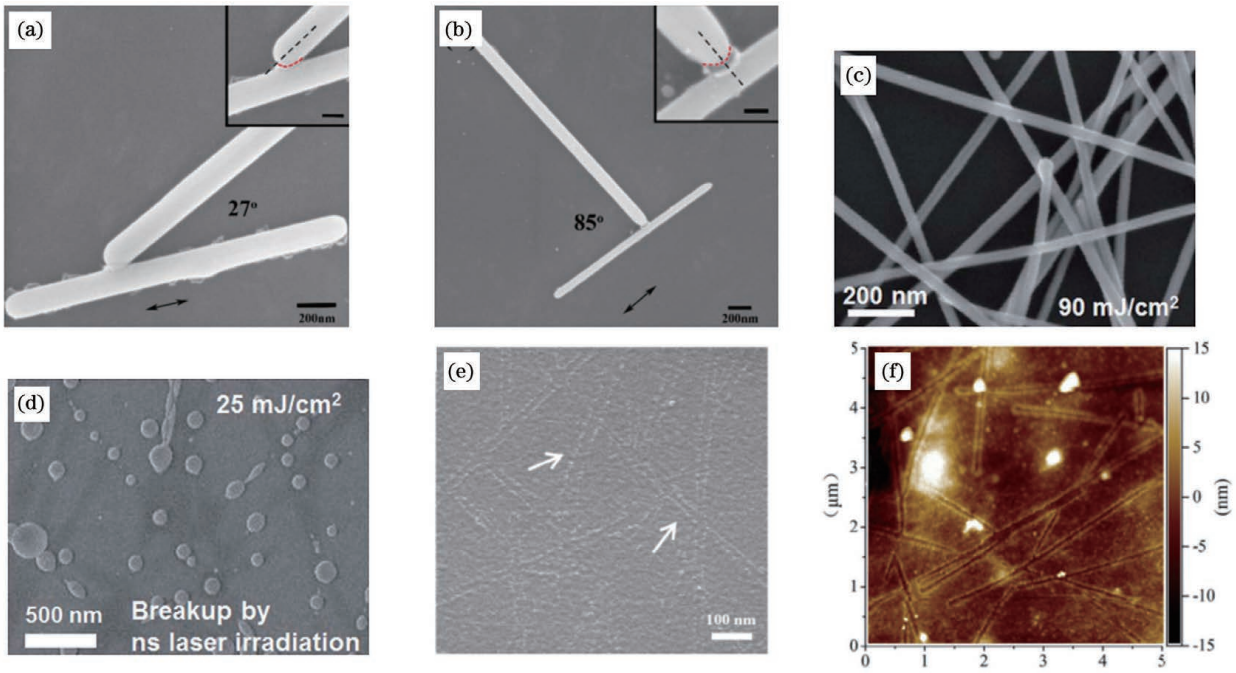

图 8 焊接后的银纳米线及衬底形貌。(a)以 27°角度连接的银纳米线[12]；(b)以 87°角度连接的银纳米线[12]；(c)飞秒激光焊接的银纳米线形貌[50]；(d)纳秒激光焊接的银纳米线形貌[50]；(e)～(f)超声清洗去除焊接纳米线后 PET 的表面微观形貌和 AFM 图[57]

Fig. 8 Morphologies of silver nanowire and substrate after welding. (a) Silver nanowires connected at angle of 27°[12]; (b) silver nanowires connected at angle of 87°[12]; (c) morphology of silver nanowires welded by femtosecond laser[50]; (d) morphology of silver nanowires welded by nanosecond laser[50]; (e)-(f) surface morphology and AFM diagram of PET after removing welded nanowires by ultrasonic cleaning[57]

由于飞秒激光辐照能在纳米线间隙处诱导局部等离子体共振，实现纳米线间的纳米连接，因此对于银纳米线形成的网状结构，可采用飞秒激光扫描实现纳米线搭接处的纳米焊接，提高银纳米线薄膜整体的导电性，使银纳米线薄膜的方块电阻降低至约 17 $\Omega\cdot sq^{-1}$，电极的透射率为 91%。为了实现器件单元的功能性，除了保证金属纳米线的有效互连外，在纳米线互连过程中也需要尽量降低对承载衬底的损伤。图 8(c)、(d)对比显示了飞秒激光与纳秒激光在银纳米线电极制造过程中对材料的损伤情况。研究表明：由于飞秒激光的“非热”加工方式以及实现银纳米线有效互连所需的功率相对较低，在较大的激光输入功率范围内焊接银纳米线时，热敏 PET(聚对苯二甲酸乙二醇酯)衬底无明显损伤且电极保持着较高的透光率；而纳秒激光焊接时，PET 衬底损伤严重。此外，如图 8(e)、(f)所示，通过空间光调制器整形，飞秒激光被整形成均匀的线光束，提高了激光焊接纳米线网格的效率。纳米线在焊接过程中部分嵌入 PET 衬

底，可以提高纳米线与衬底的黏结性[50,57]。

除金属纳米线互连外，飞秒激光在半导体一维纳米材料方面的互连也受到广泛关注[58]。如图 9 所示，利用飞秒激光辐照诱导的双光子吸收效应，并通过激子态激发产生电子空穴等离子体，能量在晶格缺陷处被俘获，使得两个纳米线连接处被局部加热和熔化，从而实现了 ZnO 纳米线的焊接。由于界面势垒减小，在偏置电压为 5 V 时，两根 ZnO 纳米线之间焊接形成的节点处的暗电导率提高了 4 个数量级[59]。上述研究证明了飞秒激光辐照实现半导体材料纳米线焊接的可行性，以及其在大面积纳米线组装和功能性纳米电子器件开发中具有广阔的应用前景。

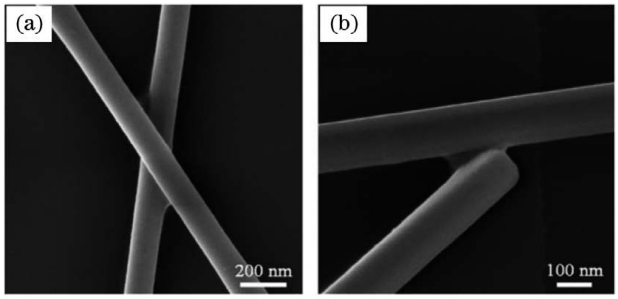

图 9 ZnO 纳米线焊接节点的微观形貌（激光能量为 77.6 mJ/cm^2，辐照时间为 30 s）[59]。(a) X 形焊接节点；(b) Y 形焊接节点

Fig. 9 Morphologies of ZnO nanowires welded joint (laser energy is 77.6 mJ/cm^2 and the irradiation time is 30 s)[59]. (a) X-shaped welded joint; (b) Y-shaped welded joint

3.2.3 异质纳米线互连

Lin 等[60]采用飞秒激光辐照使银纳米线与 TiO_2 纳米线实现了稳固连接，如图 10(a)所示，其连接机制为银纳米线与 TiO_2 纳米线搭接的节点处会产生局部电场增强，引起局部等离子体共振，从而提高了 TiO_2 纳米线的润湿性，促进了银纳米线与 TiO_2 纳米线的互连。在 Ag-TiO_2 界面处，飞秒激光辐照使 TiO_2 形成一层很薄的缺陷，这一层缺陷的存在允许界面处形成异质结，并且辐照引起的银和 TiO_2 材料结构和性能的变化仅限于节点内和节点附近区域（图 10）。

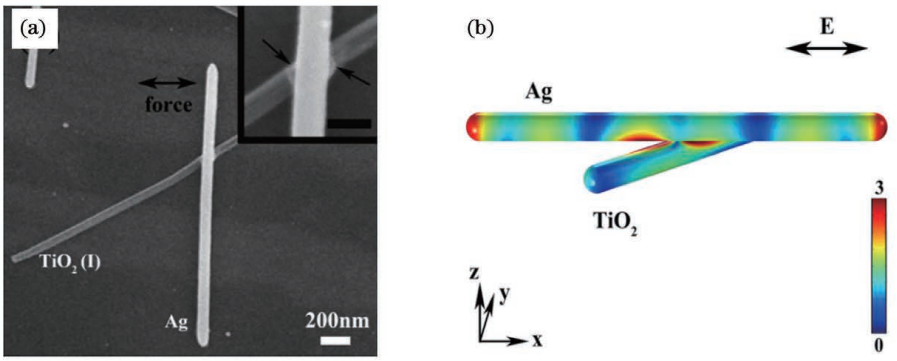

图 10 Ag-TiO_2 纳米线的形貌和场强分布[60]。(a) 17.5 mJ/cm^2 激光能量辐照下，Ag-TiO_2 纳米线形成了焊点；(b) 交叉纳米线周围的电场强度分布

Fig. 10 Morphology and field intensity distribution of Ag-TiO_2 nanowires[60]. (a) Ag-TiO_2 nanowires formed solder joint at the laser energy of 17.5 mJ/cm^2; (b) electric field intensity distribution around crossed nanowires

飞秒激光辐照也可以降低欧姆接触中 Ag-CuO 纳米线界面的肖特基势垒，实现电接触性能控制。通过可控的飞秒激光脉冲辐照使 Ag(111)纳米线和 CuO(111)纳米线界面晶格匹配，可以消除肖特基势垒。随着激光辐照时间的延长，由 Ag-CuO 纳米线异质结制备的纳米线器件从激光加工前的双肖特基势垒特性转变为整流行为[61]。Feng 等[62]利用飞秒激光辐照碳纳米纤维和银纳米线诱导形成了异质结，并且将其应用于柔性应变传感器上。由此可见，飞秒激光焊接在金属-半导体纳米级异质结器件电连接中具有广阔的应用前景。

3.2.4 一维导电材料与金属衬底互连

Lin 等[6]利用飞秒激光辐照 Au-TiO_2 纳米线结构，使金属-氧化物界面上的 TiO_2 纳米线产生局部等离子体吸收增强，进而使界面形成了具有优越力学性能和电接触性能的连接点，如图 11(a)、(b)所示。该结构可用于纳米线多层存储单元中。TiO_2 纳米线与金属电极铂(Pt)也被证实可以通过飞秒激光辐照实现互连。飞秒激光焊接的 Pt-TiO_2 纳米结构在正偏压和反向偏压下表现出不同的电性能。这种不对称电特性的产生表明了飞秒激光焊接技术对电子界面的修饰可以取代电阻开关器件中的电铸过

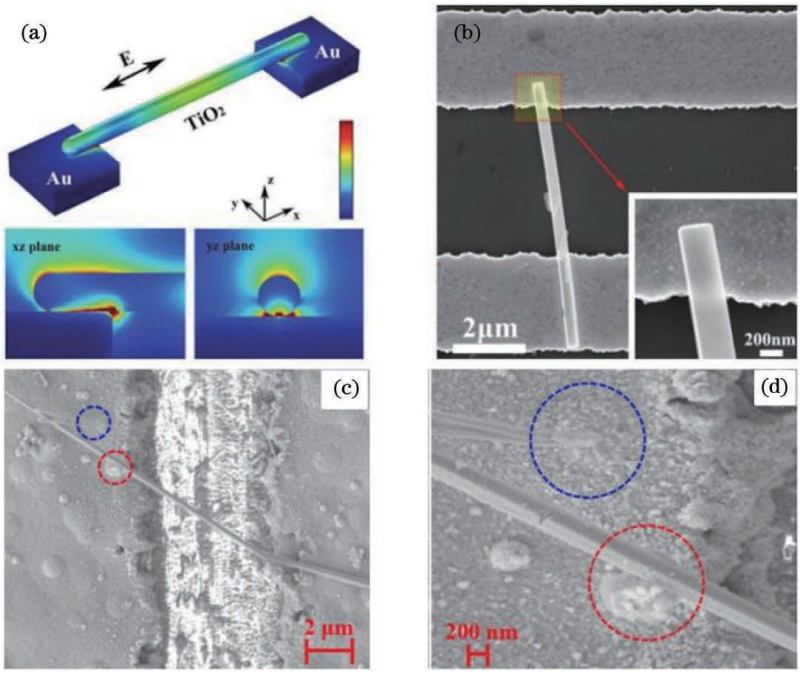

图 11 飞秒激光辐照下 Au-TiO_2 界面的场强分布及焊接形貌。(a)在 800 nm 波长偏振激光下,模拟得到的激光辐照 Au-TiO_2 纳米线连接结构周围的电场强度分布,其中双向箭头表示激光偏振方向[6];(b)经 18.3 mJ/ cm^2 飞秒激光辐照 5 s 后,Au-TiO_2 连接结构的微观图[6];(c)~(d)铜纳米线与银衬底连接后的微观形貌[64]

Fig. 11 Interfacial field intensity distribution and welding morphology of Au-TiO_2 under femtosecond laser irradiation. (a) Electric field intensity distribution around Au-TiO_2 nanowires electrode connection structure under 800 nm wavelength laser irradiation, where the double sides arrow indicates the laser polarization direction[6]; (b) microstructure of Au-TiO_2 connection structure after femtosecond laser irradiation for 5 s with energy density of 18.3 mJ/cm^2[6]; (c)-(d) microstructure of copper nanowire connected with silver substrate[64]

程,用于控制金属/氧化物界面的接触状态[63]。单根铜纳米线也可以通过飞秒激光焊接连接到银膜上,如图 11(c)、(d)所示[64];通过优化加工参数,焊接后界面处的电阻值可下降约 80%。此外,铜纳米线-碳化硅[65]、SiO_2 纳米线-碳化硅[66-67]、CuO-ZnO 纳米线与异质衬底电极也被证实可以通过飞秒激光辐照实现互连。利用该技术还可以实现碳纳米管与金属电极之间的稳定可靠连接,降低碳纳米管与电极之间的接触电阻[10,68-70]。飞秒激光焊接加工为不同金属和半导体纳米材料焊接制备肖特基势垒提供了一种有效策略。

3.2.5 导电材料的二维互连

印制电路板(PCB)的故障通常是由铜基导电路径损坏引起的。以金属纳米颗粒、导电聚合物和石墨烯等印刷材料为填料的印制电路板导电缺陷修复方法具有诸多优势,其中的激光直写还原石墨烯法具有加工分辨率高、加工方式灵活的特点,而且石墨烯具有良好的力学性能和导电性能,受到了研究人员的广泛关注。

He 等[71]使用飞秒激光直写(FsLDW)技术在柔性衬底上制备了全还原氧化石墨烯场效应晶体管(FET)。他们通过调节飞秒激光脉冲的强度来控制氧化石墨烯的含量,成功制备了导体或半导体还原氧化石墨烯的微图案,实现了源极/漏极和栅电极的直接写入,如图 12 所示。采用这种方法,在不使用任何掩模或化学试剂的情况下,成功制备出了无金属全还原氧化场效应管。全还原石墨烯器件的飞秒激光直写在石墨烯基微器件的简易制造和柔性集成方面显示出了独特的优势和巨大的发展潜力。Lim 等[72]使用飞秒激光直写将氧化石墨烯(GO)还原制备成导电石墨烯,用于修复和调整印刷电路;其制备的石墨烯的路径宽度分辨率可以达到 28.4 μm,厚度在 0.6~4.4 μm 之间可调,方块电阻最小值为 100 $\Omega \cdot sq^{-1}$。

4 超短脉冲激光加工在光互连领域的应用

以互补金属氧化物半导体(CMOS)技术为支撑

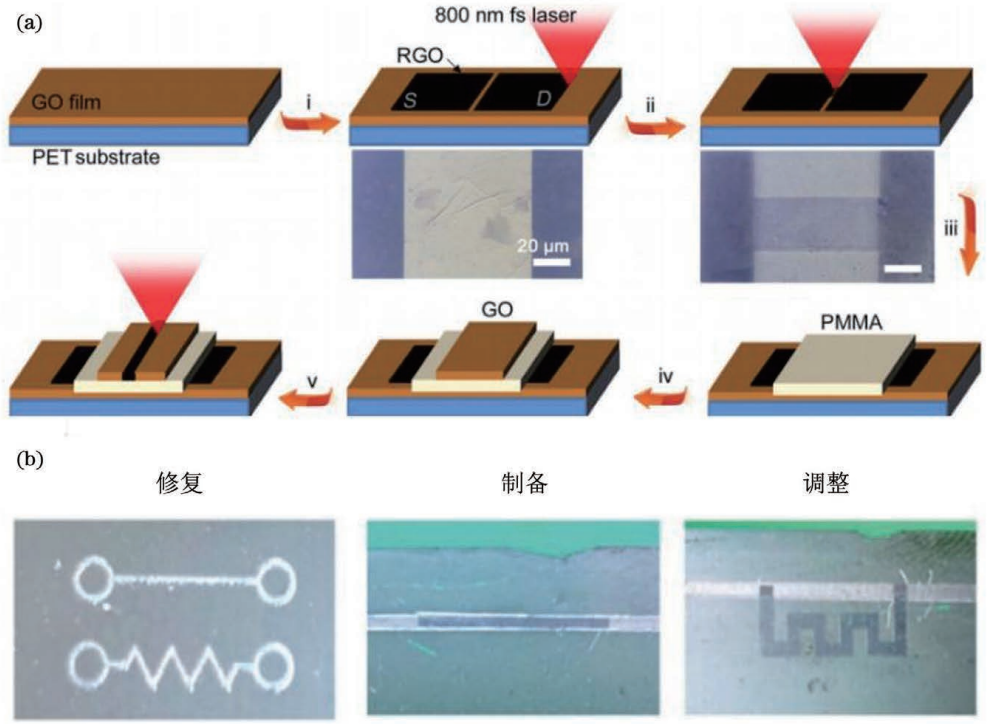

图 12 飞秒激光直写石墨烯示意图以及还原氧化石墨烯电路[71]。(a)基于飞秒激光直写技术制备全还原氧化石墨烯场效应晶体管的实验过程示意图,其中,步骤 ⅰ 为高能飞秒激光直写还原氧化石墨烯,步骤 ⅱ 为调整激光能量制备还原氧化石墨烯通道,步骤 ⅲ 为旋涂聚甲基丙烯酸甲酯 PMMA 制备介电层,步骤ⅳ为旋涂氧化石墨烯,步骤 Ⅴ 为激光直写还原氧化石墨烯制备电极;(b)制备、修复和调整后的激光直写还原氧化石墨烯电路

Fig. 12 Sketch of femtosecond laser direct writing graphene and reduced graphene oxide circuit[71]. (a) Experimental process for fabrication of fully reduced graphene oxide FET based on femtosecond laser direct writing technique, where step ⅰ represents reduction of graphene oxide by high energy femtosecond laser direct writing, step ⅱ represents preparation of reduced graphene oxide channel by adjusting laser energy, step ⅲ represents preparation of dielectric layer by spin-coating PMMA, step ⅳ represents spin-coating graphene oxide, and step Ⅴ represent preparation of electrode by reduction of graphene oxide with laser direct writing; (b) laser direct written reduced graphene oxide circuit after preparation, repair, and adjustment

的集成电路在过去半个多世纪取得了飞速发展,晶体管尺寸越来越小,集成度也越来越高,集成电路对数据的处理速度和处理能力都非常强大,而电互连的数据传输速率早已跟不上集成电路的运行速度,因此,光互连应运而生。自 20 世纪末以来,光芯片也开始发展,光芯片之间的连接需求也刺激着光互连技术的发展。从传输信道来分,光互连可以分为光纤互连、波导互连和自由空间光互连。由于芯片间或者芯片内的光互连尺寸相对较小,因此波导互连的使用最为广泛。

4.1 超快激光加工光波导

1996 年,Davis 等[73]发现聚焦飞秒激光在照射纯硅和掺锗硅等玻璃材料时,可以在材料表面或材料内部造成线条损伤,损伤区域材料的折射率变大,因此他们认为可以通过控制激光参数来改善损伤区形貌,从而可以用来引导光的传播。后来,研究人员发现,当飞秒激光照射材料时,一般会在玻璃或者聚合物中引起正折射率变化,而在晶体中引起负折射率变化。因此,利用超快激光制备的波导通常被分为三类:在飞秒激光作用下折射率增大的波导被称为Ⅰ型波导,折射率减小的波导被称为Ⅱ型波导或Ⅲ型波导,其中Ⅱ型波导以双线型波导为主,Ⅲ型波导以凹陷包层波导为主。

4.1.1 超快激光制备Ⅰ型波导

Homoelle 等[74]通过测量发现飞秒激光辐照纯硅玻璃和掺硼玻璃时可以实现 10^{-3} 量级的折射率提高。此外,可以通过调整聚焦深度[75],自上而下或自下而上地在玻璃中制备多层波导结构。Hiramatsu 等[76]在末端有 45°倒角的玻璃块中实现了 L 形波导的一次性加工,并利用该技术实现 3×8 波导阵列的加工,具体形貌如图 13(a)所示,每条波导长度均为 3.75 mm,在 1030 nm 光传输时波导的

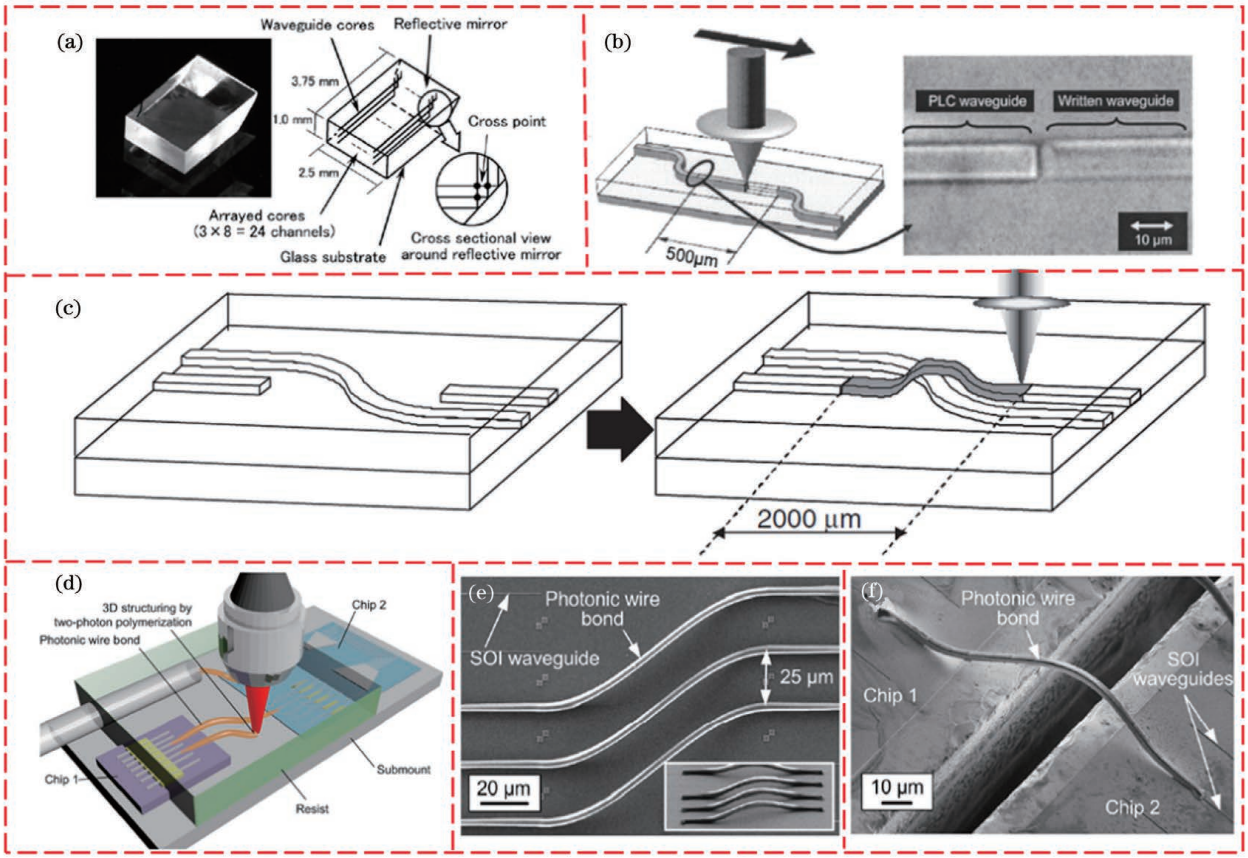

图 13 超快激光制备的Ⅰ型波导。(a)L 形波导阵列的照片和结构[76];(b)二维波导互连示意图[77];(c)三维波导互连示意图[78];(d)三维光子线的键合结构[82];(e)同一芯片上两个 SOI 波导互连[82];(f)不同芯片的互连[82]

Fig. 13 Type Ⅰ waveguide fabricated by ultrafast laser. (a) Photograph and structure of L-shaped waveguide arrays[76]; (b) two-dimensional waveguide interconnection diagram[77]; (c) three-dimensional waveguide interconnection diagram[78]; (d) three-dimensional photonic wire bonding structure[82]; (e) two SOI waveguide interconnection on the same chip[82]; (f) interconnection of different chips[82]

模场直径约为 8.3 μm,每条光路的平均传输损耗为 1.1 dB。Nasu 等[77]利用飞秒激光在由硼磷掺杂玻璃制成的平面光波导芯片(PLC)中制备了长度为 500 μm 的二维波导,如图 13(b)所示,每个耦合点的损耗仅为 0.1 dB,波导的传输损耗为 0.34 dB/cm。此外,他们还制备了长约 2 mm 的三维波导[78],如图 13(c)所示,在 1550 nm 波长处,其横向电模 TE 和横向磁模 TM 的额外损耗分别为 2.7 dB 和 2.8 dB。MacDonald 等[79]利用超快激光在硒化锌(ZnSe)晶体中制备了波导,其传输损耗为(1.07±0.03) dB/cm。Langer 等[80]用飞秒激光双光子聚合技术在聚合物材料中刻写了波导,成功实现了 PCB 板上光源和光电探测器的连接。这种方式比传统的光刻技术更加灵活,而且该波导还可以实现 Gbit/s 量级的数据传输速率。Woods 等[81]采用同样的方法实现了光源和光电二极管之间的连接。Lindenmann 等[82]在芯片内或芯片间制备光子线实现了光互连,如图 13(d)~(f)所示。该光子线在 C 波段的平均插入损耗仅为 1.6 dB,其尺寸通常为 1~2 μm,间距可以控制在 5 μm 以内。该方法适用于高密度光子线的批量生产。Lindenmann 等[83]采用相同的方法实现了多模光纤和光子芯片之间的连接,插入损耗低至 1.7 dB。Gu 等[8]利用光子线键合技术制备了聚合物波导,但两个间隔为 140 μm 的芯片连接后损耗高达 10 dB。2018 年,Billah 等[84]利用飞秒激光双光子聚合技术实现了 InP 激光器和光子芯片之间的连接,插入损耗低至 0.4 dB。

4.1.2 超快激光制备Ⅱ型波导

Ⅱ型波导主要是应力诱导型波导,目前以双线型结构的研究居多。研究人员利用飞秒激光在钽酸锂($LiTaO_3$)晶体中制备了双线型波导[85],但其退火处理之后仅能对 TM 模式产生引导,而且传输损耗较大,约为 10 dB/cm。利用超短脉冲激光传播时

自发形成的多焦点进行加工，可以在钽酸锂晶体中制备支持 TE 模式传导的双线型波导[86]。当加工材料为铌酸锂（$LiNbO_3$）晶体[87]时，虽然波导仅传输 TM 模式的光，如图 14(b)所示，但其传输损耗可降至 3 dB/cm。2020 年，He 等[88]在钽铌酸钾（KTN）晶体中制备了双线型波导，其对 632.8 nm TE 光的传输损耗仅为 0.9 dB/cm，波导形貌如图 14(a)所示。上述晶体制备的器件均与偏振相关，而利用锗酸铋[89]（$Bi_4Ge_3O_{12}$）和铜掺杂钾钠铌酸锶钡晶体（Cu∶KNSBN）[90]制备的双线型波导则呈现出与偏振无关的特性。锗酸铋晶体中的波导形貌和导光情况如图 14(c)、(d)所示。Ⅱ型波导一般情况下只能引导一种偏振模式的光传输，在互连上具有一定的局限性。虽然文献[88]和[89]也报道了与偏振无关的Ⅱ型波导，但这些波导与材料的相关性很大。

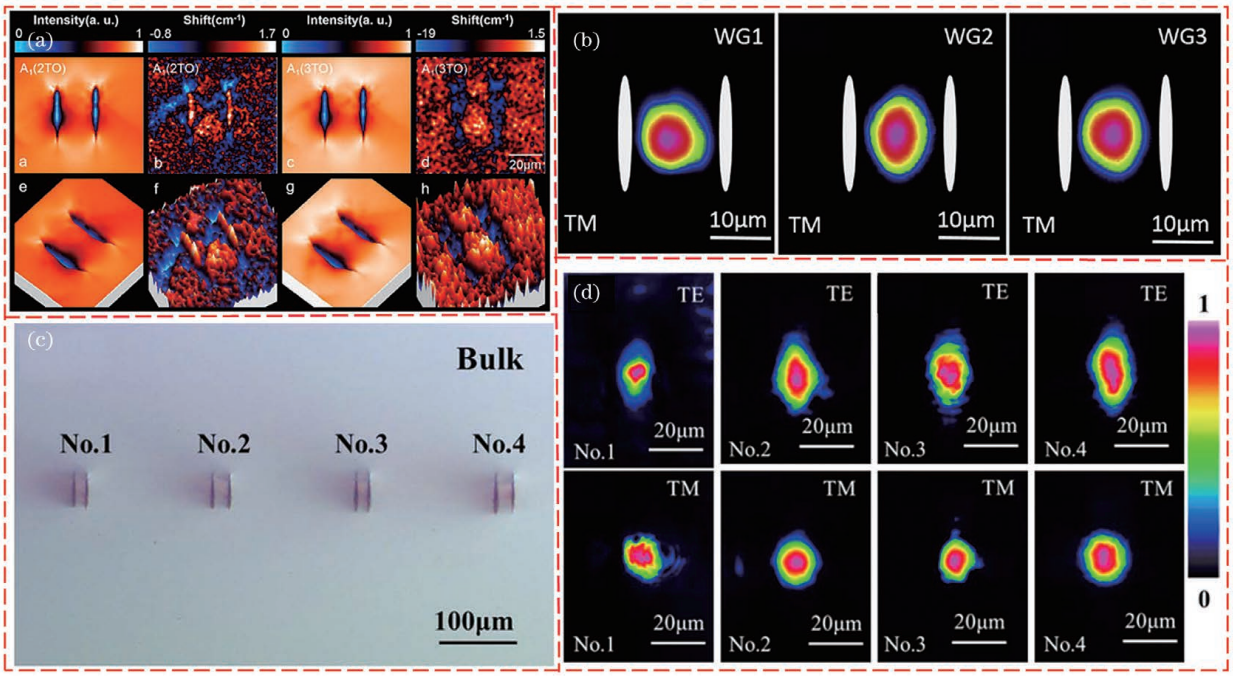

图 14 Ⅱ型波导端面的形貌及模场图。(a)在钽铌酸钾晶体中的端面形貌[88]；(b)在 z-cut MgO∶$LiNbO_3$ 晶体中的端面模场[87]；(c)在锗酸铋晶体中的端面形貌[89]；(d)在锗酸铋晶体中的端面模场[89]

Fig. 14 Morphologies and mode field diagrams of the end face of type Ⅱ waveguide. (a) End face morphologies in KTN crystal[88]; (b) end face mode field diagrams in z-cut MgO∶$LiNbO_3$ crystal[87]; (c) end face morphologies in $Bi_4Ge_3O_{12}$ crystal[89]; (d) end face mode field diagrams in $Bi_4Ge_3O_{12}$ crystal[89]

4.1.3 超快激光制备Ⅲ型波导

2013 年，He 等[89]利用飞秒激光在锗酸铋晶体中制备了凹陷包层波导，该波导与偏振无关，其退火之后的传输损耗为 2.1 dB/cm。2016 年，Lü 等[87]利用飞秒激光在铌酸锂（$LiNbO_3$）晶体中制备了凹陷包层波导，其在 632.8 nm 下的传输损耗为 0.94 dB/cm。2013 年，Xu 等[85]利用飞秒激光在钽酸锂（$LiTaO_3$）晶体中制备了凹陷包层波导，其退火处理之后的传输损耗可低至 0.38 dB/cm；在不同半径下，该波导均表现出了多模传导。为了提高加工效率，Qi 等[91]利用飞秒激光光束整形技术在铌酸锂、ZBLAN（ZrF4-BaF2-LaF3-AlF3-NaF）玻璃[92]中制备了凹陷包层波导，如图 15 所示，虽然该波导边缘不是标准的环形，但可以实现单模或多模低损耗传输，且传输特性与偏振无关。与之前单线多次扫描加工凹陷包层波导[93]相比，Qi 等采用的方法具有更高的加工效率，引入退火后处理工艺后可以进一步降低传输损耗。与Ⅱ型波导相似，Ⅲ型波导的导光区也不会受到激光辐射，这使得Ⅲ型波导不仅保持了晶体材料的原本属性，还表现出了偏振不相关性，在光互连领域展现出良好的应用前景。

4.2 超快激光加工分立元器件

分立元器件包括光源、光电探测器、光电调制器、耦合器、分束器、光开关、光放大器、光衰减器和光滤波器等。目前研究较多的是耦合器和分束器，因为这类器件本质上还是光波导的组合，其他类型的分立元器件也会随着超快激光制造能力的提升而被更多地研究。

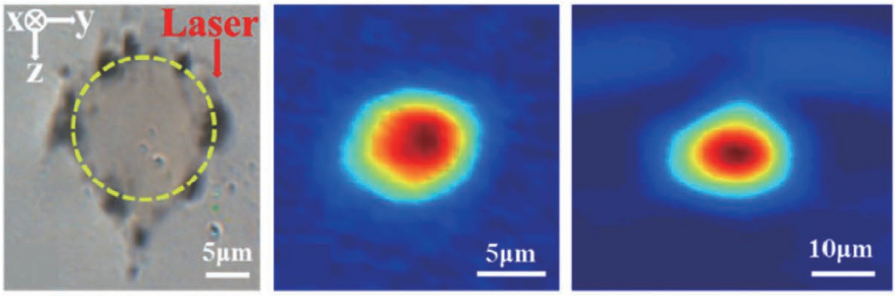

图 15 ZBLAN 晶体中Ⅲ型波导的端面形貌及模场分布[92]

Fig. 15 Morphology and mode field distributions of end face of type Ⅲ waveguide in ZBLAN crystal[92]

4.2.1 耦合器

2001 年，Minoshima 等[75]利用飞秒激光直写技术在玻璃里中制备了二维 X 形和平行波导[94]耦合器，通过调整波导的夹角、长度或间距，可以灵活地调控分光比。2002 年，Minoshima 等[95]从理论和实验两方面研究了耦合长度和波长对耦合比的影响，实验结果与耦合模理论分析结果一致。Kowalevicz 等[9]在玻璃中制备了三维 3×3 定向耦合器[96]，但由于运动平台的精度以及其他因素造成的加工误差，耦合器每个分支的光场能量并不均匀，如图 16(a)所示。Skryabin等[97]利用飞秒激光制造凹陷包层波导的方式在 Tm^{3+}∶YAG 晶体中制备了平面1×2、2×2以及三维 3×3 耦合器，如图 16(b)～(d)所示，虽然耦合比可以精确控制，但器件的插入损耗会随着分支的增加而增大。Pospiech 等[98]将飞秒激光与空间光调制器结合后实现了器件的一次性高效率扫描加工，且器件耦合比的调节范围较大。Marshall 等[3]也采用飞秒激光直写法制备了可用于光量子电路的定向耦合器。耦合比和插入损耗是耦合器的两个重要性能参数，目前超快激光加工法可以实现耦合比的精确控制，但如何降低插入损耗还需进一步研究。

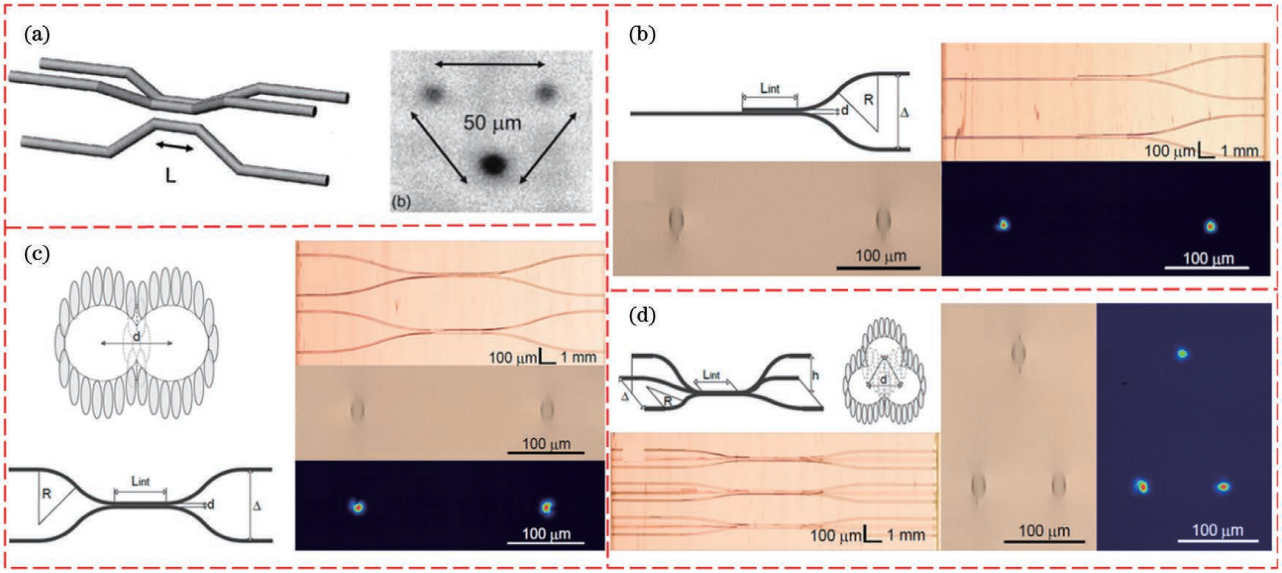

图 16 不同耦合器及其端面模场分布。(a)三维耦合器[9]；(b)1×2 耦合器[97]；(c)2×2 耦合器[97]；(d)3×3 耦合器[97]

Fig. 16 Different couplers and their end-face mode field distribution. (a) Three-dimensional coupler[9]; (b) 1×2 coupler[97]; (c) 2×2 coupler[97]; (d) 3×3 coupler[97]

4.2.2 分束器

Y 形分束器是构成复杂分束器的基本结构单元。Homoelle 等[74]利用飞秒激光在纯石英中制造了一个 Y 形分束器，当夹角为 0.5°时，其分光比接近 1∶1。Liu 等[99]制备了 1-2、1-4 和 1-8 多束分束器，如图 17(a)所示，但由于激光器功率和脉宽的不稳定以及样品运动速度的波动，能量在每个分支上并没有均匀分配。Lü 等[100]在铌酸锂晶体中制备了 1-2 和 1-4 波导分束器，随后，他们又使用制备Ⅱ型波导的方法在铌酸锂晶体中制备了分束均匀的 1-2

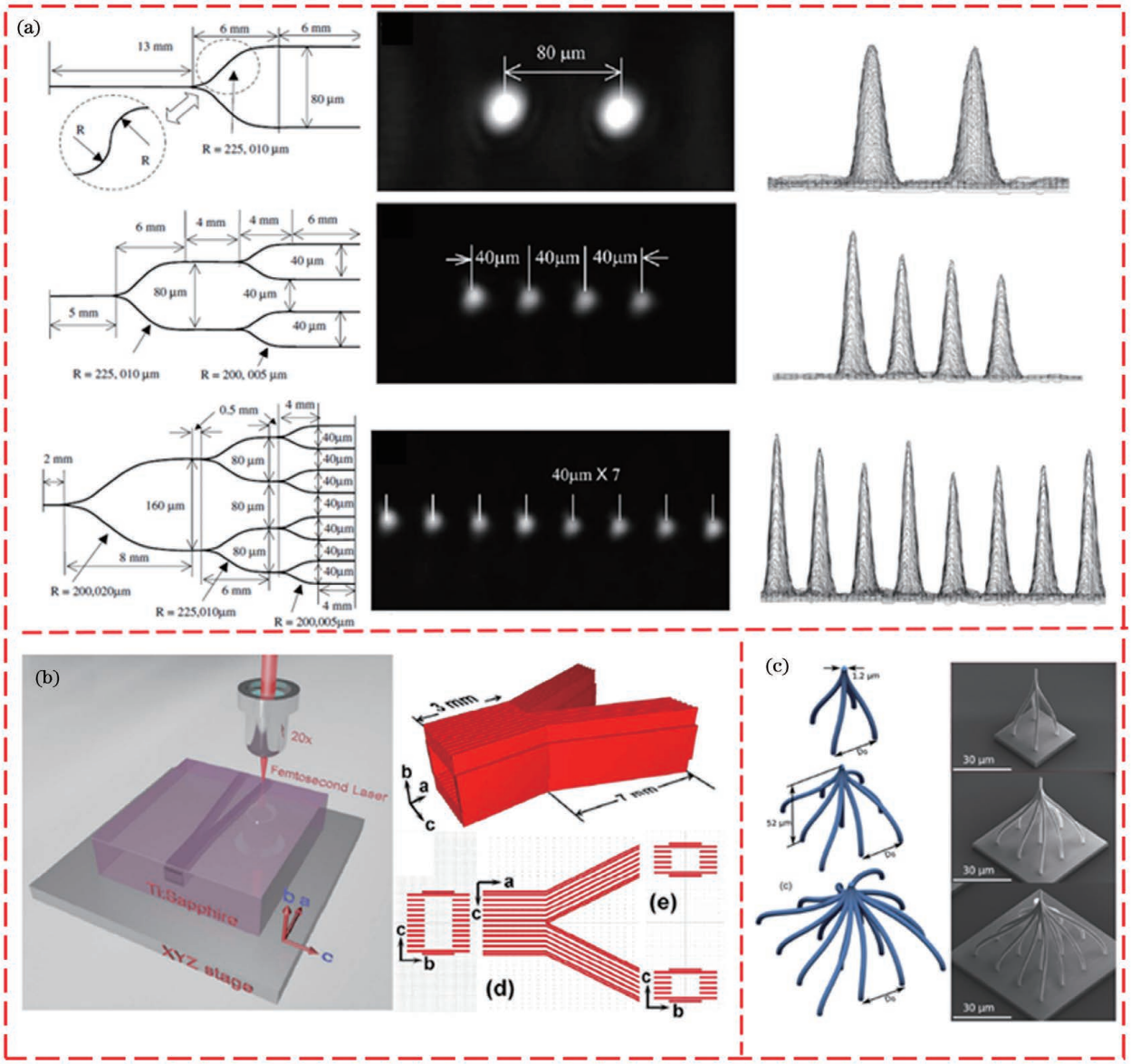

图 17 超快激光制备的分束器。(a)1-2、1-4、1-8 分束器的结构及分光情况[99];(b)基于Ⅲ型波导的 Y 分束器[104];(c)3D 打印法制备的 1-4、1-9、1-16 波导分束器[105]

Fig. 17 Beam splitters fabricated by ultrafast lasers. (a) Structure and light splitting of 1-2, 1-4, and 1-8 beam splitters[99]; (b) Y beam splitter based on type Ⅲ waveguide[104]; (c) 1-4, 1-9, and 1-16 waveguide beam splitters prepared by 3D printing method[105]

和 1-3 波导分束器,1-2、1-3 分束器的损耗分别为 1.63 dB/cm 和 2.11 dB/cm,但是该分束器只能引导 TE 模式的光[101]。Ajates 等[102]利用飞秒激光在铌酸锂晶体中制备了不同三维结构的波导分束器,并比较了每种结构对传输损耗和模态演变的影响;他们建立的数值模型可以精确预测飞秒激光在晶体中产生的折射率分布,这对于结构优化和新结构的设计具有很重要的指导意义。此外,研究人员还在钽酸锂[103]和蓝宝石晶体中[104]制备了 Y 分支波导分束器,如图 17(b)所示,其分束比接近 1∶1,且导光特性与偏振无关。

上述分束器均在介质内加工获得,飞秒激光 3D 打印技术也可以用于体外导光器件的制备。2020 年,Moughames 等[105]利用 3D 打印技术制备了 1-4、1-9 和 1-16 波导分束器,如图 17(c)所示,但其激光加工工艺窗口非常窄,当能量低于 10.4 mW 时结构不稳定,能量大于 11.2 mW 时材料会发生微炸裂。此外,该波导分束器分束的均匀性与分支波导之间的距离以及波导的表面粗糙度有关;用 632 nm 光对该分束器的性能进行测试,结果显示,

插入损耗较大，为 2.7 dB。

4.2.3 其他分立元器件

超快激光制备的微透镜和菲涅耳波带片可以在光互连中用于光束聚焦。利用飞秒激光烧蚀和化学腐蚀的方法可以在硅上制备大面积凹透镜阵列[106-107]。如图 18(a)所示，Han 等[108]通过控制激光能量、偏振态以及化学腐蚀试剂和腐蚀时间对微透镜的加工形貌实现了精确控制。Qin 等[109]通过控制飞秒脉冲延迟，制备了不同数值孔径的透镜。如图 18(b)所示，Chen 等[110]利用飞秒激光双光子聚合技术制备了菲涅耳透镜，其衍射效率可与理论极限以及商业上使用的相位棱镜相媲美。此外，他们还利用相同的技术制备了三种高衍射效率的相位分形波带片，其实测最大衍射效率分别为 20.5%、9.1%和 13%。Sun 等[111]利用飞秒激光结合化学腐蚀的方法在砷化镓(GaAs)材料上制备了菲涅耳波带片，实现了衍射和聚焦 1550 nm 红外光。此外，Kim 等[112]还在光纤端面制备了菲涅耳波带片。

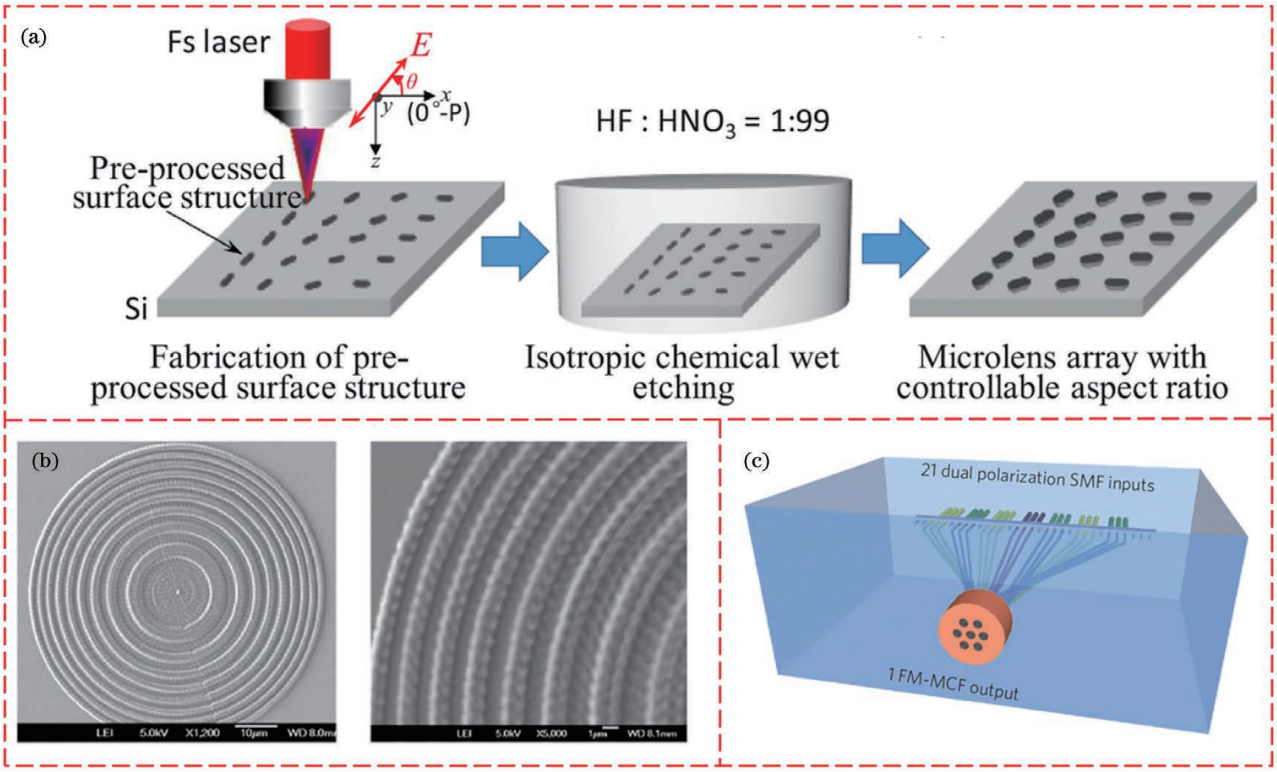

图 18 其他光分立元器件。(a)飞秒激光结合化学刻蚀制备的微透镜阵列[108]；(b)双光子聚合技术制备的菲涅耳波带片[110]；(c)多芯光纤到单模光纤的接口设备[115]

Fig. 18 Other optical discrete components. (a) Microlens array prepared by femtosecond laser combined with chemical etching[108]; (b) Fresnel zone plate prepared by two-photon polymerization technology[110]; (c) multi-core fiber to single-mode fiber interface device[115]

光纤作为最典型的光波导，在光通信领域有着广泛的应用，但是随着通信量的增加，单模光纤的传输能力即将达到上限，使用多芯光纤或多模光纤是提高通信容量的一个有效方法。为了解决多芯光纤与单模光纤的耦合问题，光纤之间的接口设备不断被提出，比如四芯光纤到单模光纤[113]、121 芯光纤到一维阵列[114]、少模多芯光纤到单模光纤[115]，如图 18(c)所示，这些接口设备可以根据多芯光纤的纤芯排列方式进行调整，制备方式非常灵活。此外，飞秒激光双光子聚合技术还可以在光纤端面制备微透镜/透镜组[116]。

5 结束语

飞秒激光实现电/光互连主要利用的是多光子还原、光动力组装、激光诱导表面等离子体共振、双光子聚合和材料相变等原理。其中：多光子还原和双光子聚合均诱导材料发生化学变化，分别生成金属材料和聚合物材料，实现电互连和光互连；光动力组装利用光驱动力操控纳米颗粒，实现材料堆积导电；激光诱导表面等离子体共振和超快激光诱导材料相变均通过使材料发生物态变化来实现焊接和折射率调制。表 1 统筹说明了超短脉冲激光在微电/

光互连领域应用所涉及到的加工方法及其优势。上述各类加工方法均涉及光子吸收、能量传递或转化、材料相变等，光、热、材料三者之间的作用机制与被加工材料、激光工艺参数等相关，通常为多种机制共同作用的结果，因此还需进一步研究。另外，虽然飞秒激光加工的最小结构可以达到亚微米级别，突破了衍射极限，但进一步减小特征尺寸、降低电阻率或传输损耗、提高抗氧化性和加工效率仍然是电/光互连面临的挑战。随着对超短脉冲激光加工的深入理解，相关技术必将在微电/光互连领域发挥更大作用。

表 1 超短脉冲激光在微电/光互连领域应用所涉及到的加工方法及其优势

Table 1 Processing methods and advantages involved in the application of ultrashort pulse laser in the field of microelectrical/optical interconnection

Processing field	Processing method	Mechanism	Material	Advantage	Application field	Reference
Electrical interconnection	Multiphoton reduction	Multiphoton absorption effect	Precursor solution	One-step processing, processing complex 3D structures	Fabrication of 2D or 3D electrical interconnect structures	[11, 15-30]
	Photodynamic assembly	Optical drive	Nanoparticle suspension	Migrating metal particles rapidly, good structural consistency	Direct writing electrode, preparation of field effect transistor, etc.	[31-44]
	Sintering method	Surface plasmon resonance	Nanoparticle ink	Direct sintering, no ion diffusion		
	Welding method	Surface plasmon resonance	Nanowire, graphene, etc	Self-limiting welding, no thermal damage to the substrate	Flexible display, flexible sensor, memristor, electrode repair, etc.	[53-71]
Optical interconnection	Modification method	Refractive index change	Transparent medium such as glass	Machining directly on or inside the material	Three dimensional optical waveguide, coupler, beam splitter, etc.	[74-80, 85-93]
	Two-photon polymerization	Two-photon absorption effect	Polymer solution	Flexible preparation, processing complex 3D structures		[80, 84, 110, 116]

参 考 文 献

[1] Xu B B, Zhang D D, Liu X Q, et al. Fabrication of microelectrodes based on precursor doped with metal seeds by femtosecond laser direct writing[J]. Optics Letters, 2014, 39(3): 434-437.

[2] Xu B B, Zhang R, Wang H, et al. Laser patterning of conductive gold micronanostructures from nanodots[J]. Nanoscale, 2012, 4(22): 6955-6958.

[3] Marshall G D, Politi A, Matthews J C F, et al. Laser written waveguide photonic quantum circuits [J]. Optics Express, 2009, 17(15): 12546-12554.

[4] Garnett E C, Cai W S, Cha J J, et al. Self-limited plasmonic welding of silver nanowire junctions[J]. Nature Materials, 2012, 11(3): 241-249.

[5] Han S, Hong S, Ham J, et al. Fast plasmonic laser nanowelding for a Cu-nanowire percolation network for flexible transparent conductors and stretchable electronics[J]. Advanced Materials, 2014, 26(33): 5808-5814.

[6] Lin L C, Liu L, Musselman K, et al. Plasmonic-radiation-enhanced metal oxide nanowire heterojunctions for controllable multilevel memory [J]. Advanced Functional Materials, 2016, 26(33): 5979-5986.

[7] 王联甫, 丁烨, 王根旺, 等. 激光诱导微纳连接技

术研究进展[J/OL]. 机械工程学报: 1-12. [2021-12-01]. http://kns.cnki.net/kcms/detail/11.2187.TH.20211102.1615.040.html.
Wang L F, Ding Y, Wang G W, et al. Research advances of laser-induced micro-nano joining technology [J/OL]. Journal of Mechanical Engineering: 1-12. [2021-12-01]. http://kns.cnki.net/kcms/detail/11.2187.TH.20211102.1615.040.html.

[8] Gu Z C, Amemiya T, Ishikawa A, et al. Optical transmission between III-V chips on Si using photonic wire bonding[J]. Optics Express, 2015, 23(17): 22394-22403.

[9] Kowalevicz A M, Sharma V, Ippen E P, et al. Three-dimensional photonic devices fabricated in glass by use of a femtosecond laser oscillator[J]. Optics Letters, 2005, 30(9): 1060-1062.

[10] Cui J L, Cheng Y, Zhang J W, et al. Femtosecond laser irradiation of carbon nanotubes to metal electrodes[J]. Applied Sciences, 2019, 9(3): 476.

[11] Elles C G, Shkrob I A, Crowell R A, et al. Excited state dynamics of liquid water: insight from the dissociation reaction following two-photon excitation [J]. The Journal of Chemical Physics, 2007, 126(16): 164503.

[12] Lin L C, Liu L, Peng P, et al. *In situ* nanojoining of Y- and T-shaped silver nanowires structures using femtosecond laser radiation [J]. Nanotechnology, 2016, 27(12): 125201.

[13] 任笑莹, 崔健磊, 陆洋, 等. 基于纳米连接的互连结构的电/力学性能研究进展[J]. 中国激光, 2021, 48(8): 0802021.
Ren X Y, Cui J L, Lu Y, et al. Research progress on electrical/mechanical properties of interconnection structures based on nanowelding [J]. Chinese Journal of Lasers, 2021, 48(8): 0802021.

[14] Serbin J, Egbert A, Ostendorf A, et al. Femtosecond laser-induced two-photon polymerization of inorganic-organic hybrid materials for applications in photonics[J]. Optics Letters, 2003, 28(5): 301-303.

[15] Dey G R, El Omar A K, Jacob J A, et al. Mechanism of trivalent gold reduction and reactivity of transient divalent and monovalent gold ions studied by gamma and pulse radiolysis [J]. The Journal of Physical Chemistry A, 2011, 115(4): 383-391.

[16] Belloni J, Mostafavi M, Remita H, et al. Radiation-induced synthesis of mono- and multi-metallic clusters and nanocolloids [J]. New Journal of Chemistry, 1998, 22(11): 1239-1255.

[17] Li C, Hu J, Jiang L, et al. Shaped femtosecond laser induced photoreduction for highly controllable Au nanoparticles based on localized field enhancement and their SERS applications [J]. Nanophotonics, 2020, 9(3): 691-702.

[18] Tanaka T, Ishikawa A, Kawata S. Two-photon-induced reduction of metal ions for fabricating three-dimensional electrically conductive metallic microstructure[J]. Applied Physics Letters, 2006, 88(8): 081107.

[19] Ishikawa A, Tanaka T, Kawata S. Improvement in the reduction of silver ions in aqueous solution using two-photon sensitive dye [J]. Applied Physics Letters, 2006, 89(11): 113102.

[20] Cao Y Y, Takeyasu N, Tanaka T, et al. 3D metallic nanostructure fabrication by surfactant-assisted multiphoton-induced reduction[J]. Small, 2009, 5(10): 1144-1148.

[21] Cao Y Y, Dong X Z, Takeyasu N, et al. Morphology and size dependence of silver microstructures in fatty salts-assisted multiphoton photoreduction microfabrication[J]. Applied Physics A, 2009, 96(2): 453-458.

[22] Lu W E, Zhang Y L, Zheng M L, et al. Femtosecond direct laser writing of gold nanostructures by ionic liquid assisted multiphoton photoreduction [J]. Optical Materials Express, 2013, 3(10): 1660-1673.

[23] Ren X L, Zheng M L, Jin F, et al. Laser direct writing of silver nanowire with amino acids-assisted multiphoton photoreduction [J]. The Journal of Physical Chemistry C, 2016, 120(46): 26532-26538.

[24] Xu B B, Xia H, Niu L G, et al. Flexible nanowiring of metal on nonplanar substrates by femtosecond-laser-induced electroless plating[J]. Small, 2010, 6(16): 1762-1766.

[25] Nakamura R, Hitomi M, Kinashi K, et al. Two-photon excitation by femtosecond laser in poly(*N*-vinylpyrrolidone) matrix doped with silver ions[J]. Chemical Physics Letters, 2013, 558: 62-65.

[26] Baldacchini T, Pons A C, Pons J, et al. Multiphoton laser direct writing of two-dimensional silver structures[J]. Optics Express, 2005, 13(4): 1275-1280.

[27] Maruo S, Saeki T. Femtosecond laser direct writing of metallic microstructures by photoreduction of silver nitrate in a polymer matrix [J]. Optics Express, 2008, 16(2): 1174-1179.

[28] Shukla S, Vidal X, Furlani E P, et al. Subwavelength direct laser patterning of conductive

gold nanostructures by simultaneous photopolymerization and photoreduction [J]. ACS Nano, 2011, 5(3): 1947-1957.

[29] Blasco E, Müller J, Müller P, et al. Fabrication of conductive 3D gold-containing microstructures via direct laser writing[J]. Advanced Materials, 2016, 28(18): 3592-3595.

[30] Hu Q, Sun X Z, Parmenter C D J, et al. Additive manufacture of complex 3D Au-containing nanocomposites by simultaneous two-photon polymerisation and photoreduction [J]. Scientific Reports, 2017, 7: 17150.

[31] Wang H, Liu S, Zhang Y L, et al. Controllable assembly of silver nanoparticles induced by femtosecond laser direct writing [J]. Science and Technology of Advanced Materials, 2015, 16(2): 024805.

[32] 陈忠赟, 方淦, 曹良成, 等. 飞秒激光光镊直写银微纳结构[J]. 中国激光, 2018, 45(4): 0402006.
Chen Z Y, Fang G, Cao L C, et al. Direct writing of silver micro-nanostructures by femtosecond laser tweezer[J]. Chinese Journal of Lasers, 2018, 45(4): 0402006.

[33] Urban A S, Lutich A A, Stefani F D, et al. Laser printing single gold nanoparticles[J]. Nano Letters, 2010, 10(12): 4794-4798.

[34] Bahns J T, Sankaranarayanan S K R S, Giebink N C, et al. Optically directed mesoscale assembly and patterning of electrically conductive organic-inorganic hybrid structures[J]. Advanced Materials, 2012, 24(35): OP242-OP246.

[35] Son Y, Yeo J, Ha C W, et al. Application of the specific thermal properties of Ag nanoparticles to high-resolution metal patterning[J]. Thermochimica Acta, 2012, 542: 52-56.

[36] Huang H, Sivayoganathan M, Duley W W, et al. High integrity interconnection of silver submicron/nanoparticles on silicon wafer by femtosecond laser irradiation [J]. Nanotechnology, 2015, 26(2): 025303.

[37] Huang H, Sivayoganathan M, Duley W W, et al. Efficient localized heating of silver nanoparticles by low-fluence femtosecond laser pulses [J]. Applied Surface Science, 2015, 331: 392-398.

[38] Son Y, Yeo J, Moon H, et al. Nanoscale electronics: digital fabrication by direct femtosecond laser processing of metal nanoparticles[J]. Advanced Materials, 2011, 23(28): 3176-3181.

[39] Noh J, Kim D. Femtosecond laser sintering of silver nanoparticles for conductive thin-film fabrication [J]. Applied Physics A, 2020, 126(2): 124.

[40] Mizoshiri M, Arakane S, Sakurai J, et al. Direct writing of Cu-based micro-temperature detectors using femtosecond laser reduction of CuO nanoparticles[J]. Applied Physics Express, 2016, 9(3): 036701.

[41] Mizoshiri M, Hata S. Selective fabrication of p-type and n-type thermoelectric micropatterns by the reduction of CuO/NiO mixed nanoparticles using femtosecond laser pulses [J]. Applied Physics A, 2017, 124(1): 64.

[42] 廖嘉宁, 王欣达, 周兴汶, 等. 铜纳米颗粒的飞秒激光连接过程研究[J]. 中国激光, 2021, 48(8): 0802008.
Liao J N, Wang X D, Zhou X W, et al. Joining process of copper nanoparticles with femtosecond laser irradiation [J]. Chinese Journal of Lasers, 2021, 48(8): 0802008.

[43] Huang Y J, Xie X Z, Li M N, et al. Copper circuits fabricated on flexible polymer substrates by a high repetition rate femtosecond laser-induced selective local reduction of copper oxide nanoparticles [J]. Optics Express, 2021, 29(3): 4453-4463.

[44] Mizoshiri M, Yoshidomi K. Cu patterning using femtosecond laser reductive sintering of CuO nanoparticles under inert gas injection[J]. Materials, 2021, 14(12): 3285.

[45] 丁铠文, 王聪, 罗志, 等. 超快激光光束整形原理与方法及其在功能性微结构制造中的应用[J]. 中国激光, 2021, 48(2): 0202005.
Ding K W, Wang C, Luo Z, et al. Principle and method of ultrafast laser beam shaping and its application in functional microstructure fabrication [J]. Chinese Journal of Lasers, 2021, 48(2): 0202005.

[46] 孔德键, 孙小燕, 董卓林, 等. 飞秒激光空间光束整形加工技术研究进展[J]. 激光与光电子学进展, 2020, 57(11): 111416.
Kong D J, Sun X Y, Dong Z L, et al. Progress in femtosecond laser processing technology based on space beam shaping [J]. Laser & Optoelectronics Progress, 2020, 57(11): 111416.

[47] Liu Y, Zhang J M, Gao H, et al. Capillary-force-induced cold welding in silver-nanowire-based flexible transparent electrodes [J]. Nano Letters, 2017, 17(2): 1090-1096.

[48] Hu H, Wang Z Y, Ye Q X, et al. Substrateless welding of self-assembled silver nanowires at air/water interface [J]. ACS Applied Materials & Interfaces, 2016, 8(31): 20483-20490.

[49] Huang Y L, Tian Y H, Hang C J, et al. Self-limited nanosoldering of silver nanowires for high-

performance flexible transparent heaters[J]. ACS Applied Materials & Interfaces, 2019, 11(24): 21850-21858.

[50] Ha J, Lee B J, Hwang D J, et al. Femtosecond laser nanowelding of silver nanowires for transparent conductive electrodes[J]. RSC Advances, 2016, 6(89): 86232-86239.

[51] Hu Y W, Liang C, Sun X Y, et al. Enhancement of the conductivity and uniformity of silver nanowire flexible transparent conductive films by femtosecond laser-induced nanowelding[J]. Nanomaterials, 2019, 9(5): 673.

[52] Liang C, Sun X Y, Zheng J F, et al. Surface ablation thresholds of femtosecond laser micropatterning silver nanowires network on flexible substrate[J]. Microelectronic Engineering, 2020, 232: 111396.

[53] Ghenuche P, Cherukulappurath S, Taminiau T H, et al. Spectroscopic mode mapping of resonant plasmon nanoantennas[J]. Physical Review Letters, 2008, 101(11): 116805.

[54] Liu L, Peng P, Hu A M, et al. Highly localized heat generation by femtosecond laser induced plasmon excitation in Ag nanowires[J]. Applied Physics Letters, 2013, 102(7): 073107.

[55] Hu A, Deng G L, Courvoisier S, et al. Femtosecond laser induced surface melting and nanojoining for plasmonic circuits[J]. Proceedings of SPIE, 2013, 8809: 880907.

[56] Lin L, Huang H, Sivayoganathan M, et al. Assembly of silver nanoparticles on nanowires into ordered nanostructures with femtosecond laser radiation[J]. Applied Optics, 2015, 54(9): 2524-2531.

[57] Liang C, Sun X Y, Su W M, et al. Fast welding of silver nanowires for flexible transparent conductive film by spatial light modulated femtosecond laser[J]. Advanced Engineering Materials, 2021, 23(12): 2100584.

[58] 肖宇, 霍金鹏, 孙天鸣, 等. p 型氧化铜纳米线的飞秒激光纳米连接[J]. 中国激光, 2021, 48(8): 0802005.
Xiao Y, Huo J P, Sun T M, et al. Nanojoining of p-type copper oxide nanowires using femtosecond laser[J]. Chinese Journal of Lasers, 2021, 48(8): 0802005.

[59] Xing S L, Lin L C, Zou G S, et al. Two-photon absorption induced nanowelding for assembling ZnO nanowires with enhanced photoelectrical properties[J]. Applied Physics Letters, 2019, 115(10): 103101.

[60] Lin L C, Zou G S, Liu L, et al. Plasmonic engineering of metal-oxide nanowire heterojunctions in integrated nanowire rectification units[J]. Applied Physics Letters, 2016, 108(20): 203107.

[61] Xiao M, Lin L, Xing S, et al. Nanojoining and tailoring of current-voltage characteristics of metal-p type semiconductor nanowire heterojunction by femtosecond laser irradiation[J]. Journal of Applied Physics, 2020, 127(18): 184901.

[62] Feng J Y, Tian Y H, Wang S M, et al. Femtosecond laser irradiation induced heterojunctions between carbon nanofibers and silver nanowires for a flexible strain sensor[J]. Journal of Materials Science & Technology, 2021, 84: 139-146.

[63] Xing S L, Lin L C, Zou G S, et al. Improving the electrical contact at a Pt/TiO_2 nanowire interface by selective application of focused femtosecond laser irradiation[J]. Nanotechnology, 2017, 28(40): 405302.

[64] Deng Y B, Bai Y F, Yu Y C, et al. Laser nanojoining of copper nanowires[J]. Journal of Laser Applications, 2019, 31(2): 022414.

[65] Yu Y C, Deng Y B, Al Hasan M A, et al. Femtosecond laser-induced non-thermal welding for a single Cu nanowire glucose sensor[J]. Nanoscale Advances, 2020, 2(3): 1195-1205.

[66] Xing S L, Lin L C, Huo J P, et al. Plasmon-induced heterointerface thinning for Schottky barrier modification of core/shell SiC/SiO_2 nanowires[J]. ACS Applied Materials & Interfaces, 2019, 11(9): 9326-9332.

[67] Lin L C, Huo J P, Peng P, et al. Contact engineering of single core/shell SiC/SiO_2 nanowire memory unit with high current tolerance using focused femtosecond laser irradiation[J]. Nanoscale, 2020, 12(9): 5618-5626.

[68] 孙天鸣, 肖宇, 霍金鹏, 等. 飞秒激光辐照连接金属氧化物纳米线及电性能调控[J]. 中国激光, 2021, 48(8): 0802006.
Sun T M, Xiao Y, Huo J P, et al. Nanojoining and electrical performance modulation of metal oxide nanowires based on femtosecond laser irradiation[J]. Chinese Journal of Lasers, 2021, 48(8): 0802006.

[69] Mei H H, Cheng Y, Wang H J, et al. Femtosecond laser-induced interconnection of multi-walled carbon nanotubes[J]. Ferroelectrics, 2019, 548(1): 50-59.

[70] 梅欢欢, 崔健磊, 程杨, 等. 碳纳米管与金属电极异质连接及其电学性能的研究进展[J]. 中国激光, 2021, 48(8): 0802023.

Mei H H, Cui J L, Cheng Y, et al. Heterogeneous connection of carbon nanotubes with metal electrodes and its electrical properties[J]. Chinese Journal of Lasers, 2021, 48(8): 0802023.

[71] He Y, Zhu L, Liu Y, et al. Femtosecond laser direct writing of flexible all-reduced graphene oxide FET[J]. IEEE Photonics Technology Letters, 2016, 28(18): 1996-1999.

[72] Lim C H J, Sandeep C S S, Murukeshan V M, et al. Direct laser writing of graphene-based electrical interconnects for printed circuit board repair[J]. Advanced Materials Technologies, 2021, 6(12): 2100514.

[73] Davis K M, Miura K, Sugimoto N, et al. Writing waveguides in glass with a femtosecond laser[J]. Optics Letters, 1996, 21(21): 1729-1731.

[74] Homoelle D, Wielandy S, Gaeta A L, et al. Infrared photosensitivity in silica glasses exposed to femtosecond laser pulses[J]. Optics Letters, 1999, 24(18): 1311-1313.

[75] Minoshima K, Kowalevicz A M, Hartl I, et al. Photonic device fabrication in glass by use of nonlinear materials processing with a femtosecond laser oscillator[J]. Optics Letters, 2001, 26(19): 1516-1518.

[76] Hiramatsu S, Mikawa T, Ibaragi O, et al. Laser-written optical-path redirected waveguide device for optical back-plane interconnects[J]. IEEE Photonics Technology Letters, 2004, 16(9): 2075-2077.

[77] Nasu Y, Kohtoku M, Hibino Y. Low-loss waveguides written with a femtosecond laser for flexible interconnection in a planar light-wave circuit [J]. Optics Letters, 2005, 30(7): 723-725.

[78] Nasu Y, Kohtoku M, Hibino Y, et al. Three-dimensional waveguide interconnection in planar lightwave circuits by direct writing with femtosecond laser[J]. Japanese Journal of Applied Physics, 2005, 44(48): L1446-L1448.

[79] MacDonald J R, Thomson R R, Beecher S J, et al. Ultrafast laser inscription of near-infrared waveguides in polycrystalline ZnSe [J]. Optics Letters, 2010, 35(23): 4036-4038.

[80] Langer G, Satzinger V, Schmidt V, et al. PCB with fully integrated optical interconnects[J]. Proceedings of SPIE, 2011, 7944: 794408.

[81] Woods R, Feldbacher S, Zidar D, et al. Development and characterization of optoelectronic circuit boards produced by two-photon polymerization using a polysiloxane containing acrylate functional groups [J]. Applied Optics, 2013, 52(3): 388-393.

[82] Lindenmann N, Balthasar G, Hillerkuss D, et al. Photonic wire bonding: a novel concept for chip-scale interconnects[J]. Optics Express, 2012, 20 (16): 17667-17677.

[83] Lindenmann N, Dottermusch S, Goedecke M L, et al. Connecting silicon photonic circuits to multicore fibers by photonic wire bonding[J]. Journal of Lightwave Technology, 2015, 33(4): 755-760.

[84] Billah M R, Blaicher M, Hoose T, et al. Hybrid integration of silicon photonics circuits and InP lasers by photonic wire bonding[J]. Optica, 2018, 5(7): 876-883.

[85] Xu M M, He R Y, Sun S Q, et al. Femtosecond laser micromachined optical waveguides in $LiTaO_3$ crystal [J]. Physica Status Solidi (RRL)-Rapid Research Letters, 2013, 7(11): 1014-1017.

[86] Li L Q, Nie W J, Li Z Q, et al. Femtosecond laser writing of optical waveguides by self-induced multiple refocusing in $LiTaO_3$ crystal[J]. Journal of Lightwave Technology, 2019, 37(14): 3452-3458.

[87] Lü J M, Cheng Y Z, Lu Q M, et al. Femtosecond laser written optical waveguides in z-cut MgO∶$LiNbO_3$ crystal: fabrication and optical damage investigation[J]. Optical Materials, 2016, 57: 169-173.

[88] He S, Yang Q X, Zhang B, et al. A waveguide mode modulator based on femtosecond laser direct writing in KTN crystals[J]. Results in Physics, 2020, 18: 103307.

[89] He R Y, An Q, Vázquez de Aldana J R, et al. Femtosecond-laser micromachined optical waveguides in $Bi_4Ge_3O_{12}$ crystals [J]. Applied Optics, 2013, 52(16): 3713-3718.

[90] Nie W J, de Aldana J R V, Chen F. Dual-line optical waveguides in Cu∶KNSBN crystal fabricated by direct femtosecond laser writing [J]. Optical Engineering, 2015, 54: 097106.

[91] Qi J, Wang P, Liao Y, et al. Fabrication of polarization-independent single-mode waveguides in lithium niobate crystal with femtosecond laser pulses [J]. Optical Materials Express, 2016, 6(8): 2554-2559.

[92] Zhang Q, Yang D, Qi J, et al. Single scan femtosecond laser transverse writing of depressed cladding waveguides enabled by three-dimensional focal field engineering[J]. Optics Express, 2017, 25(12): 13263-13270.

[93] Okhrimchuk A, Mezentsev V, Shestakov A, et al. Low loss depressed cladding waveguide inscribed in YAG∶Nd single crystal by femtosecond laser pulses

[J]. Optics Express, 2012, 20(4): 3832-3843.

[94] Streltsov A M, Borrelli N F. Fabrication and analysis of a directional coupler written in glass by nanojoule femtosecond laser pulses[J]. Optics Letters, 2001, 26(1): 42-43.

[95] Minoshima K, Kowalevicz A, Ippen E, et al. Fabrication of coupled mode photonic devices in glass by nonlinear femtosecond laser materials processing[J]. Optics Express, 2002, 10(15): 645-652.

[96] Suzuki K, Sharma V, Fujimoto J G, et al. Characterization of symmetric [3 × 3] directional couplers fabricated by direct writing with a femtosecond laser oscillator [J]. Optics Express, 2006, 14(6): 2335-2343.

[97] Skryabin N, Kalinkin A, Dyakonov I, et al. Femtosecond laser written depressed-cladding waveguide 2×2, 1×2 and 3×3 directional couplers in Tm^{3+} : YAG crystal[J]. Micromachines, 2019, 11(1): 1.

[98] Pospiech M, Emons M, Steinmann A, et al. Double waveguide couplers produced by simultaneous femtosecond writing [J]. Optics Express, 2009, 17(5): 3555-3563.

[99] Liu J R, Zhang Z Y, Chang S D, et al. Directly writing of 1-to-*N* optical waveguide power splitters in fused silica glass using a femtosecond laser[J]. Optics Communications, 2005, 253(4/5/6): 315-319.

[100] Lü J M, Cheng Y Z, Yuan W H, et al. Three-dimensional femtosecond laser fabrication of waveguide beam splitters in $LiNbO_3$ crystal [J]. Optical Materials Express, 2015, 5(6): 1274-1280.

[101] Lü J M, Cheng Y Z, Vázquez de Aldana J R, et al. Femtosecond laser writing of optical-lattice-like cladding structures for three-dimensional waveguide beam splitters in $LiNbO_3$ crystal [J]. Journal of Lightwave Technology, 2016, 34(15): 3587-3591.

[102] Ajates J G, Vázquez deAldana J R, Chen F, et al. Three-dimensional beam-splitting transitions and numerical modelling of direct-laser-written near-infrared $LiNbO_3$ cladding waveguides [J]. Optical Materials Express, 2018, 8(7): 1890-1901.

[103] Cheng C, Romero C, de Aldana J R V, et al. Superficial waveguide splitters fabricated by femtosecond laser writing of $LiTaO_3$ crystal [J]. Optical Engineering, 2015, 54(6): 067113.

[104] Ren Y Y, Zhang L M, Xing H G, et al. Cladding waveguide splitters fabricated by femtosecond laser inscription in Ti : sapphire crystal [J]. Optics & Laser Technology, 2018, 103: 82-88.

[105] Moughames J, Porte X, Larger L, et al. 3D printed multimode-splitters for photonic interconnects [J]. Optical Materials Express, 2020, 10(11): 2952-2961.

[106] Du G Q, Yang Q, Chen F, et al. Direct fabrication of seamless roller molds with gapless and shaped-controlled concave microlens arrays [J]. Optics Letters, 2012, 37(21): 4404-4406.

[107] Deng Z F, Yang Q, Chen F, et al. Fabrication of large-area concave microlens array on silicon by femtosecond laser micromachining[J]. Optics Letters, 2015, 40(9): 1928-1931.

[108] Han W N, Han Z H, Yuan Y P, et al. Continuous control of microlens morphology on Si based on the polarization-dependent femtosecond laser induced periodic surface structures modulation[J]. Optics & Laser Technology, 2019, 119: 105629.

[109] Qin B, Li X W, Yao Z L, et al. Fabrication of microlenses with continuously variable numerical aperture through a temporally shaped femtosecond laser[J]. Optics Express, 2021, 29(3): 4596-4606.

[110] Chen Q D, Wu D, Niu L G, et al. Phase lenses and mirrors created by laser micronanofabrication via two-photon photopolymerization[J]. Applied Physics Letters, 2007, 91(17): 171105.

[111] Sun X Y, Zhou F, Dong X R, et al. Fabrication of GaAs micro-optical components using wet etching assisted femtosecond laser ablation [J]. Journal of Modern Optics, 2020, 67(20): 1516-1523.

[112] Kim J, Ha W, Park J, et al. Micro Fresnel zone plate lens inscribed on a hard polymer clad fiber using femtosecond pulsed laser[J]. IEEE Photonics Technology Letters, 2013, 25(8): 761-763.

[113] Thomson R R, Bookey H T, Psaila N D, et al. Ultrafast-laser inscription of a three dimensional fan-out device for multicore fiber coupling applications [J]. Optics Express, 2007, 15(18): 11691-11697.

[114] Thomson R R, Harris R J, Birks T A, et al. Ultrafast laser inscription of a 121-waveguide fan-out for astrophotonics[J]. Optics Letters, 2012, 37(12): 2331-2333.

[115] van Uden R G H, Correa R A, Lopez E A, et al. Ultra-high-density spatial division multiplexing with a few-mode multicore fibre[J]. Nature Photonics, 2014, 8(11): 865-870.

[116] Gissibl T, Thiele S, Herkommer A, et al. Two-photon direct laser writing of ultracompact multi-lens objectives[J]. Nature Photonics, 2016, 10(8): 554-560.

Application of Ultrashort Pulse Laser Manufacturing in Microelectrical/Optical Interconnection

Sun Xiaoyan[1,2], Liang Chang[1,2], Zhang Wei[1,2], Kong Dejian[1,2], Feng Yuting[1,2], Hu Youwang[1,2*], Duan Ji'an[1,2]

[1] *College of Mechanical and Electrical Engineering, Central South University, Changsha* 410083, *Hunan, China;*
[2] *State Key Laboratory of High Performance Complex Manufacturing, Changsha* 410083, *Hunan, China*

Abstract

Objective Significance electronic and information devices are becoming increasingly miniaturized and portable with technological advancements. These advancements require high-density distribution of device function units. This introduces new challenges to the electrical and optical interconnection technology among function units. Some techniques such as photolithography and electron beam have been developed for fabricating microelectrical and micro-optical devices. Although these methods have high resolution, they are inflexible for three-dimensional (3D) fabrication. Ultrafast pulse lasers are a versatile tool for fabricating microelectrical/optical devices owing to their high resolution, minimal thermal effect, and flexibility. In this study, we briefly introduce the basic mechanism of ultrashort pulse lasers for microelectrical/optical interconnection, including multiphoton-induced reduction, surface plasmon resonant, and two-photon photopolymerization. Furthermore, this study focuses on the application of ultrafast laser manufacturing in microelectrical/optical interconnection.

Progress According to different applications, femtosecond laser interconnect technology can be categorized into electrical and optical interconnections. Between them, electrical interconnection technology can be used to connect zero-, one-, and two-dimensional nanomaterials.

For zero-dimensional nanomaterials, ultrafast laser-induced interconnection mechanisms include multiphoton reduction, photodynamic assembly, and selective laser sintering. Multiphoton reduction is a high-resolution approach for 3D electrical interconnection owing to the multiple absorptions induced in the metal-ion precursor (Fig. 1). To improve the quality of electrical structures, surfactant (Fig. 2) or polymeric matrix (Fig. 3) is added to the precursor to avoid the diffusion of ions. In addition, photodynamic assembly for electrical interconnection is developed to address the diffusion of metal ions in the precursor. This method uses laser-driven force to capture and connect nanoparticles (Fig. 4). Furthermore, selective laser sintering can be used to fabricate patterned electrodes in the atmosphere using surface plasma resonance (Fig. 5).

In nanowire electrical interconnection, femtosecond laser-induced local plasma resonance can be used to weld homogeneous nanowires or nanowires and substrate. Studies have shown that local-field enhancement appears at the ends of nanowires or coupled gap regions during femtosecond laser irradiation, inducing localized plasmon resonance to generate localized high temperatures, which can be used for nanowire joining, cutting, or reshaping. For example, silver nanowire networks will have local plasma resonance at junctions during femtosecond laser irradiation, resulting in a localized high temperature, to realize nanowire welding and reduce the sheet resistance of silver nanowire transparent conductive films (Figs. 7 and 8). The welding between heterogeneous material interfaces can also be realized to form electrical interconnection using local plasmon resonance induced via femtosecond lasers, such as Ag-TiO_2 nanowire welding and TiO_2 nanowire-Au electrode welding (Fig. 12). In two-dimensional material electrical interconnection, femtosecond laser direct writing induced reduction of graphene oxide can be used for electrode repairing or adjustment. To realize one- and two-dimensional material electrical interconnection, femtosecond laser has the advantages of small thermal impact, almost no thermal damage occurs to substrates, and high processing resolution. Therefore, the method of welding nanomaterials using femtosecond laser irradiation has important application prospects in developing flexible electronic devices and functional micro-nano devices.

In optical interconnection, femtosecond laser modification processing can often induce refractive index changes in glass and crystalline materials. Two-photon polymerization can be used for additive manufacturing outside the base material, which can process complex 3D structures compared with femtosecond laser modification(Fig. 13). The annealing treatment after modification processing can effectively reduce the transmission loss of a waveguide; beam

shaping technology can improve the processing efficiency of the waveguide. However, efforts are still required to improve the compatibility of waveguide manufacturing. Among discrete components, relatively simple couplers, beam splitters, and microlenses have been extensively studied. However, further research is required to fabricate complex devices such as on-chip light source, modulator, and detector component.

Conclusion and Prospect Electrical/optical interconnection can be realized via femtosecond laser irradiation primarily through the principles of photon reduction, photodynamic assembly, laser-induced surface plasmon resonance, two-photon polymerization, or material phase transition. The interconnection process is complex, involving photon absorption, energy transfer or transformation, material phase transformation, etc. Laser processing involves the interaction between light, heat and materials. The welding of materials is usually the result of a combination of various mechanisms; therefore, further research is required. In addition, the smallest structure size can reach the submicron level. However, further reducing the characteristic size, reducing resistivity or transmission loss, and improving oxidation resistance and processing efficiency are still the challenges faced by the electrical/optical interconnection. With more understanding of ultrashort pulse laser processing, related technologies will play a more important role in the field of microelectrical/optical interconnection.

Key words laser technique; ultrashort pulse laser; multiphoton induced reduction; surface plasmon resonant; two-photon photopolymerization; optical waveguide